Nuclear Physics under the low-energy, high intensity frontier

Photon vortex generation using high power laser and the effect on nuclear reactions

QST T. Hayakawa

Collaborations

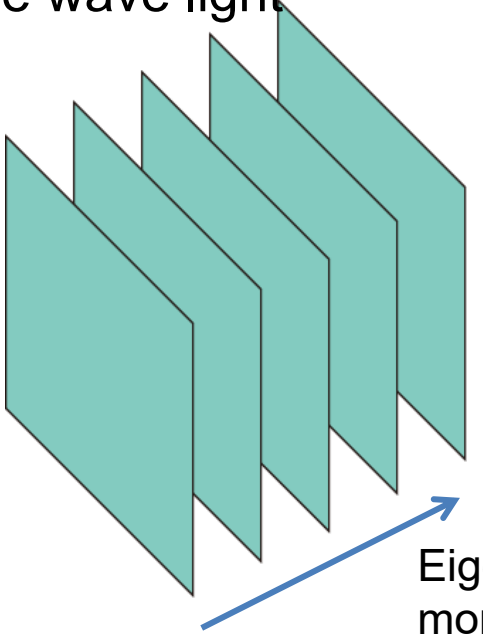
T. Maruyama, T. Kajino, M.-K. Cheoun

T. Maruyama has done almost all calculation.

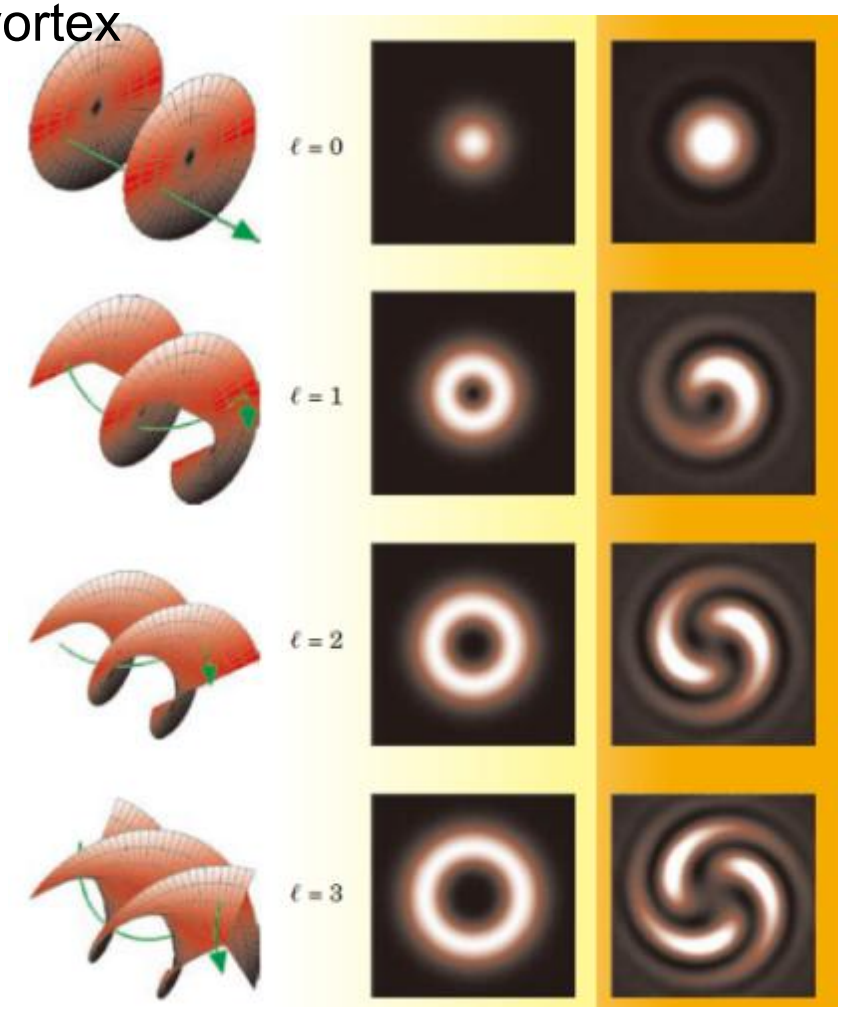
T. Maruyama, T. Hayakawa, T. Kajino, Sci. Rep. 9, 51 (2019)
T. Maruyama, T. Hayakawa, T. Kajino, Sci. Rep. 9, 7998 (2019)
T. Maruyama, T. Hayakawa, M.K.Cheoun, T.Kajino, PLB826, 136779 (2022)
T. Maruyama, T. Hayakawa, M.K.Cheoun, T.Kajino, Phys. Rev. Research 5, 043289 (2023).
T. Maruyama, T. Hayakawa, M.K.Cheoun, T.Kajino, ApJ 975, 51 (2024)
Effect of Photon Vortex Generated in Extremely Strong Magnetic Fields on Stellar Nucleosynthesis
T. Maruyama, T. Hayakawa, M.K.Cheoun, T.Kajino, Phys. Rev. D 111, 016016 (2025).
Photon vortex generation from nonlinear Compton scattering in Feynman approach

Optical vortex

Plane wave light



Optical vortex



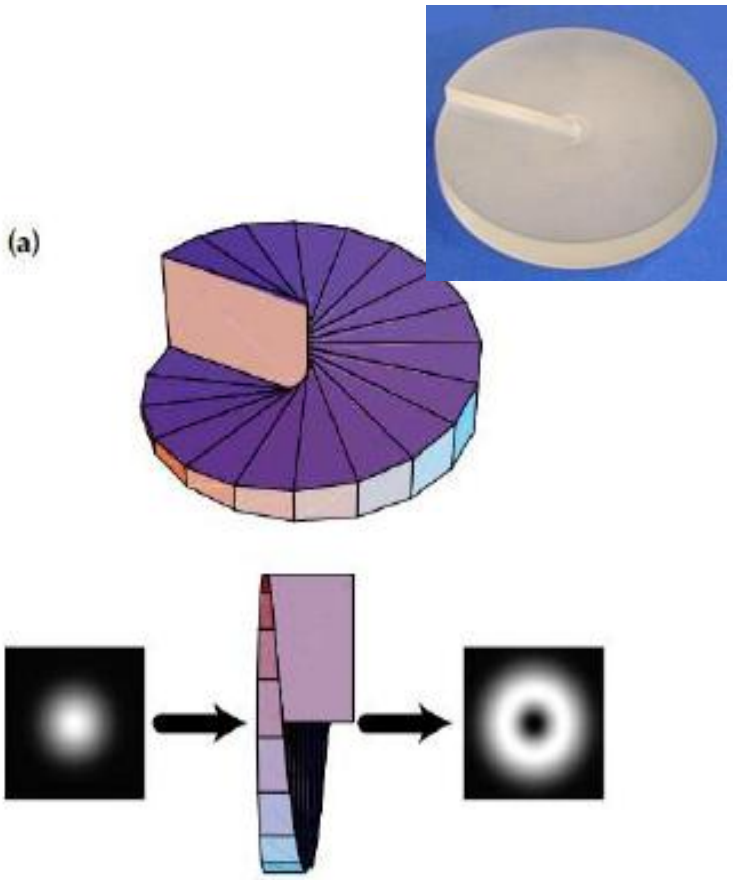
L. Allen, et al. Phys. Rev. A, 45, 8185 (1992)

They showed that the possibility of "photon vortex" in addition to "light vortex".

M. Padgett et al., Phys. Today 57 (2004) 35

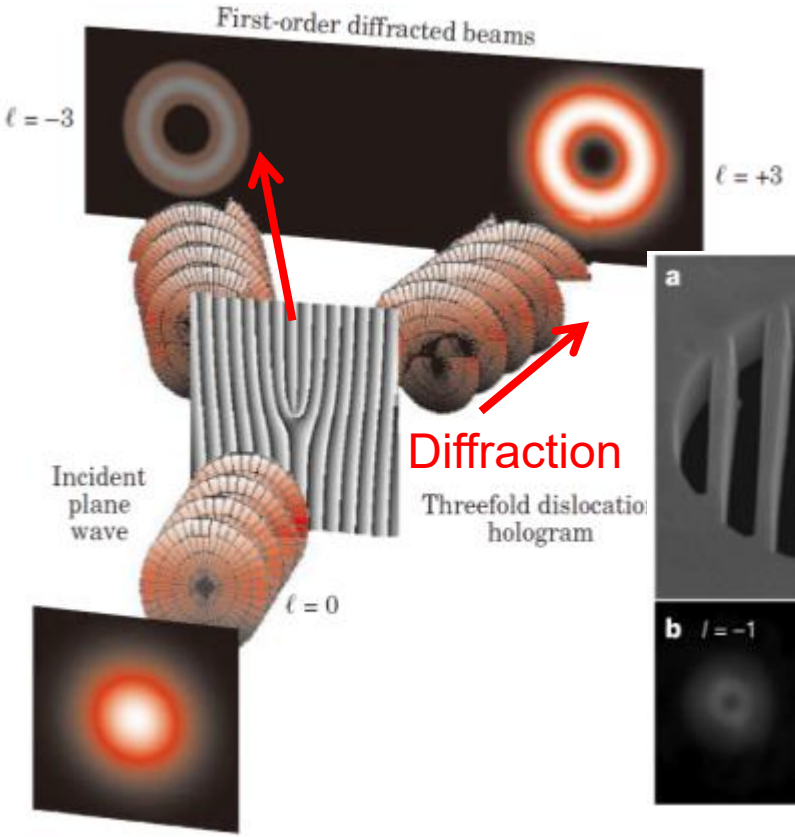
Optical vortex generation by optical methods

Spiral phase plate

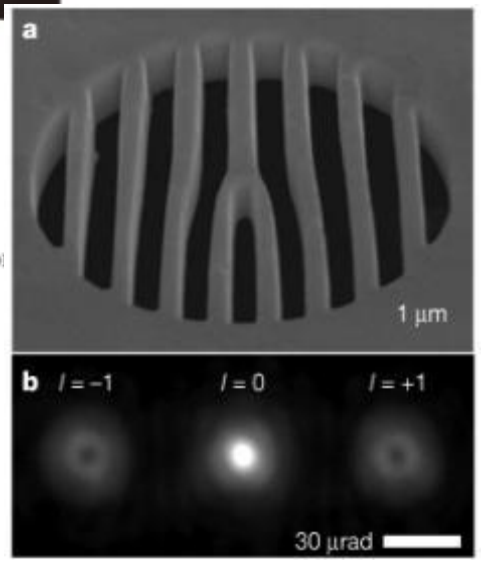


J. Courtial, K. O'Holleran, Eur. Phys. J.
Special Topics 145, 35 (2007)

Holographic phase plate



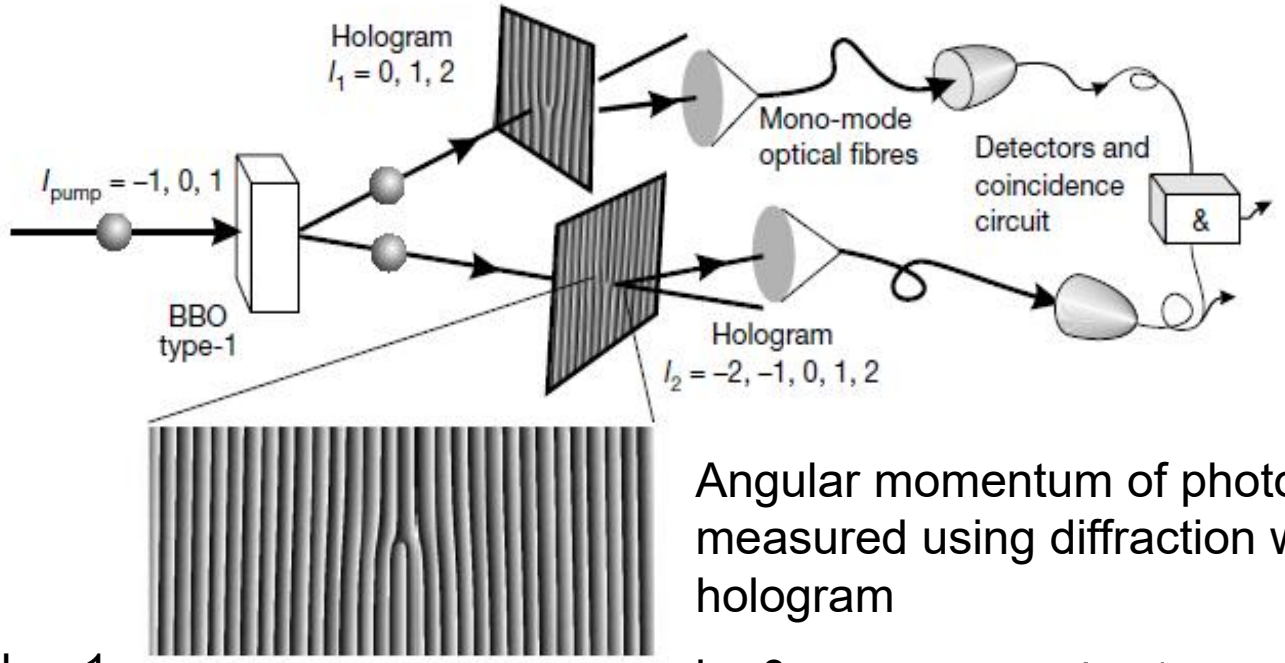
M. Padgett et al., Phys. Today 57 (2004) 35



Phase dislocation aperture

J. Verbeeck, et al. Nature, 467, 301 (2010).

Verification of "photon vortex" using quantum entanglement



Entanglement of the orbital angular momentum states of photons

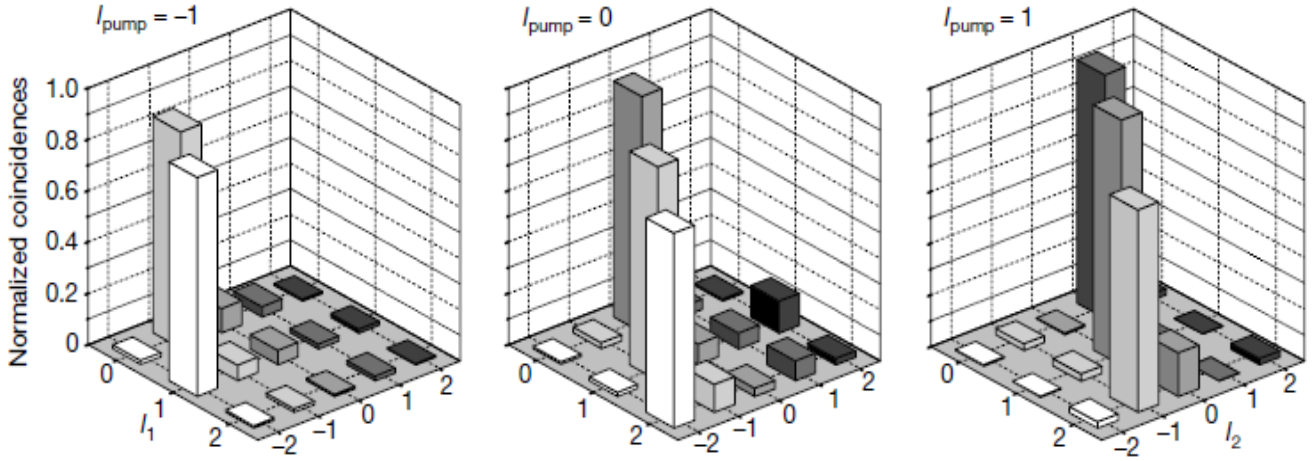
A. Mair et al. Nature, 412, 313 (2001).

Angular momentum of photon is measured using diffraction with hologram

l = -1

l = 0

l = 1



Result shows that the sum of the angular momenta is conserved.

nature physics

LETTERS

PUBLISHED ONLINE: 13 FEBRUARY 2011 | DOI: 10.1038/NPHYS1907

Twisting of light around rotating black holes

Fabrizio Tamburini[1], Bo Thidé[2]*, Gabriel Molina-Terriza[3] and Gabriele Anzolin[4]

Kerr black holes are among the most intriguing predictions of Einstein's general relativity theory[1,2]. These rotating massive astrophysical objects drag and intermix their surrounding space and time, deflecting and phase-modifying light emitted near them. We have found that this leads to a new relativistic effect that imprints orbital angular momentum on such light.

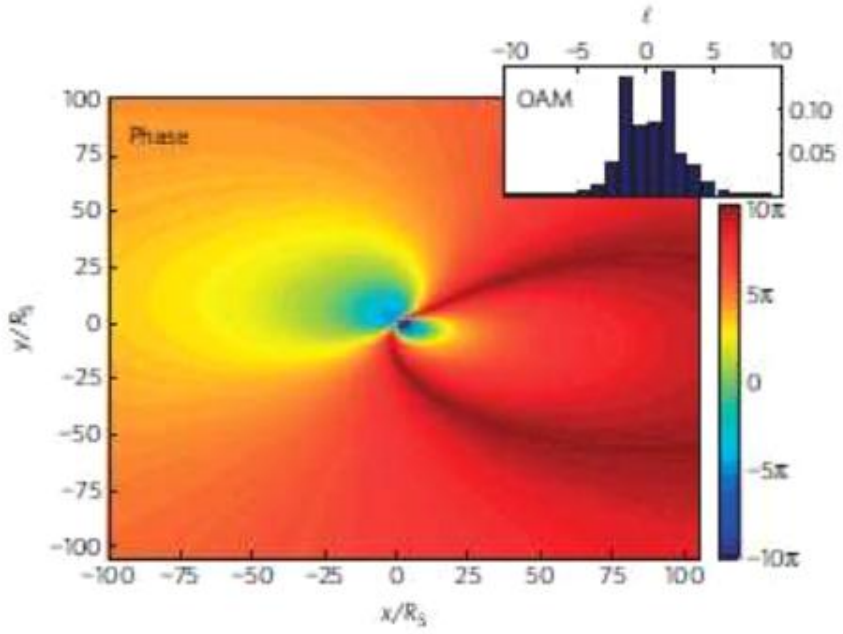
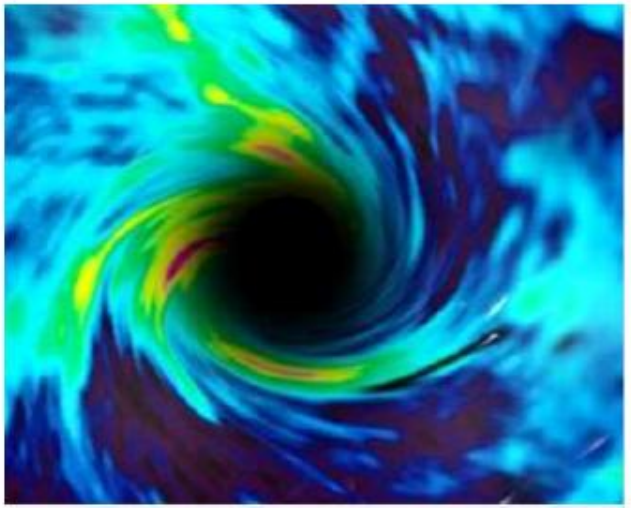


Figure 1 | Total phase variation of light generated in a region of size $100R_S \times 100R_S$ in the equatorial xy plane of a quasi-extremal rotating black hole ($a = 0.99$) as seen by an asymptotic observer. This region of



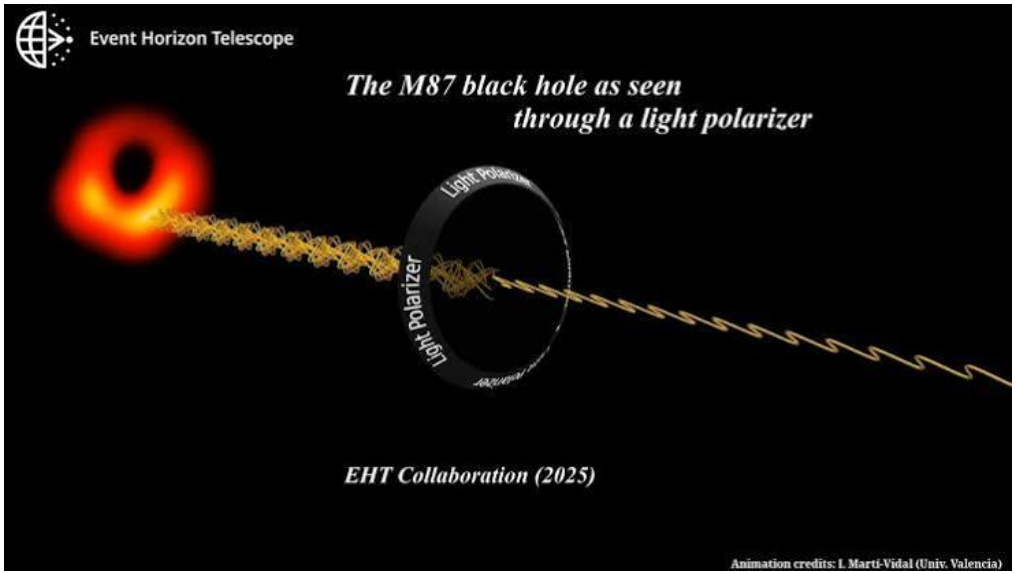
Black holes put a twist on light passing by.

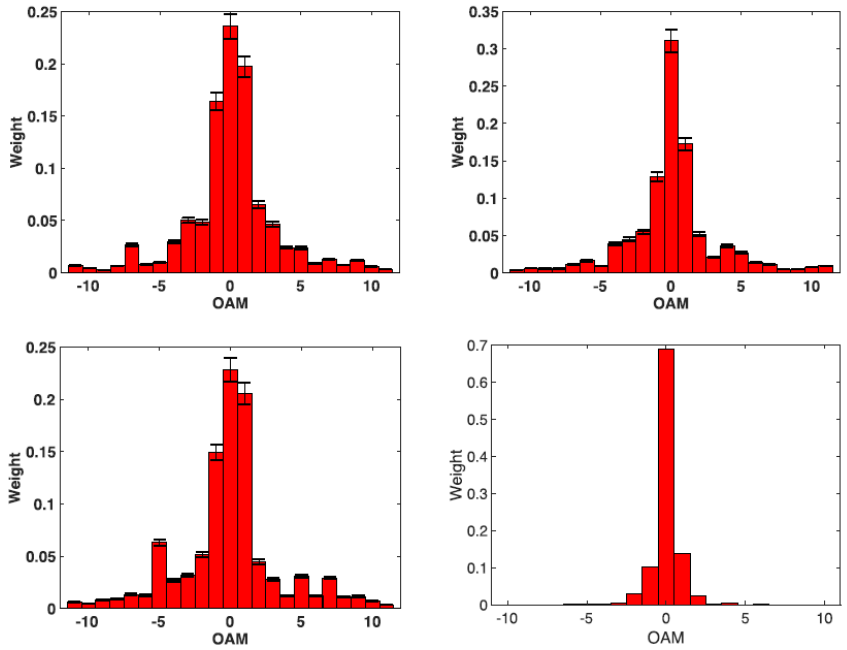
Fabrizio Tamburini

13 February 2011 | Nature | doi:10.1038/news.2011.90

Astronomical observation of photon vortex

"Measurement of the spin of the M87 black hole from its observed twisted light",
F. Tamburini, et al. MNRAS 492, L22–L27 (2020)



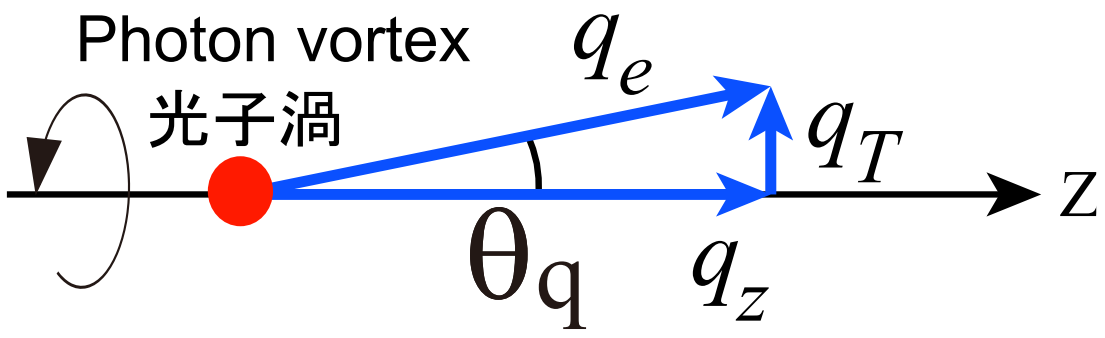


Observation of optical vortex from black hole!

The M87 rotates clockwise with an estimated rotation parameter a = 0.90 ± 0.05
with an ~ 95 per cent confidence level (c.l.)

Feature of photon vortex

1. The photon vortex has a nonzero q_T



2. The photon vortex is the eigenstate of the z-component of the total angular momentum, Jz.

Wave-function of Laguerre-Gaussian

$$\nabla^2 \boldsymbol{E} - \frac{1}{c^2}\frac{\partial^2 \boldsymbol{E}}{\partial t^2} = 0 \qquad \left(\nabla_T^2 + 2ik\frac{\partial}{\partial z}\right)u = 0$$

When $\dfrac{\partial^2 A}{\partial z^2} \ll k\dfrac{\partial A}{\partial z}$

$$\boldsymbol{A}_i(\boldsymbol{r}) = \frac{\boldsymbol{\epsilon}_i(h_i)}{\sqrt{2k}} u(\boldsymbol{r}) e^{-ikt}$$

$$u(\boldsymbol{r}) = \sqrt{\frac{2}{\pi R_z}}\frac{1}{w(z)} G\left[|L|, p, \frac{2r}{w(z)}\right] \exp\left\{i\left[L\phi + kz + \frac{zr^2}{z_R w^2(z)} - (2p + |L| + 1)\theta_G\right]\right\} \quad (1)$$

with

$$G\left[|L|, p, x\right] = \sqrt{\frac{p!}{\pi(|L|+p)!}}\left(\frac{x}{\sqrt{2}}\right)^{|L|} e^{-x^2/4}\mathcal{L}_p^{|L|}\left(\frac{x^2}{2}\right),$$

$$\theta_G = \tan^{-1}\left(\frac{z}{z_R}\right), \quad w(z) = w_0\sqrt{1 + z^2/z_R^2}, \qquad z_R = kw_0^2/2, \quad (2)$$

L :angular momentum $\mathcal{L}_p^{|L|}$:Laguerre function W_0 :radius

Wave-function of Bessel photons

Adding A_z for Gauge $\nabla \cdot \boldsymbol{A} = 0$

$$\boldsymbol{A}_{Lh}(\boldsymbol{r}; q_z, k) \propto e^{i(q_z z - e_q t)} \left[q_z J_L(q_T r) e^{iL\phi}, ihq_z J_L(q_T r) e^{iL\phi}, ihq_T J_{L+h}(q_T r) e^{i(L+h)\phi} \right]$$

$\boldsymbol{A}(h = +1)$ & $\boldsymbol{A}(h = -1)$ are not orthogonal

We take two states as eigen states

$\boldsymbol{A}(h = +1) - \boldsymbol{A}(h = -1)$ TM-mode

$\boldsymbol{A}(h = +1) + \boldsymbol{A}(h = -1)$ TE-mode

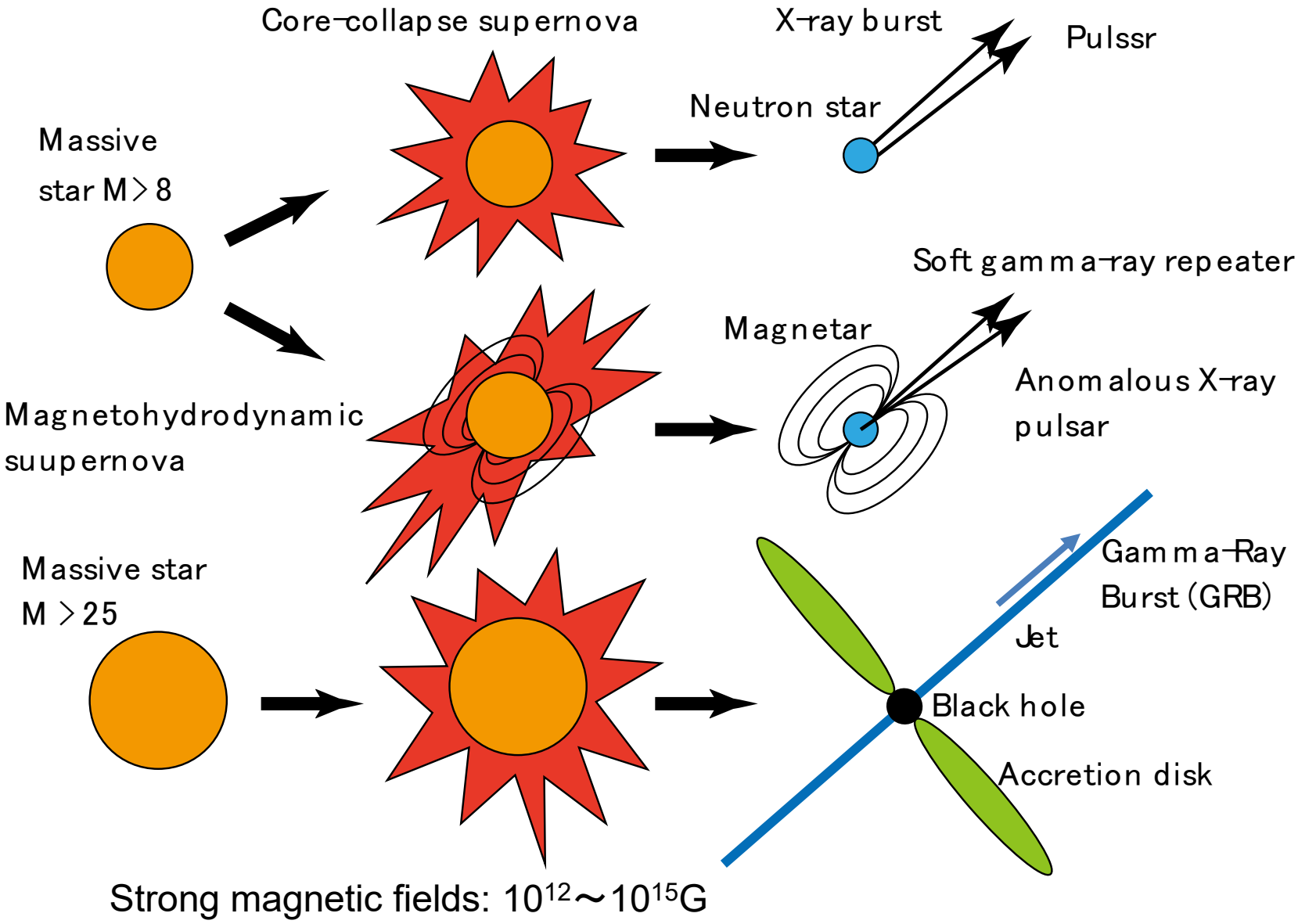
Final photon wave-functon

$$\boldsymbol{A}_K^{(1)} = \frac{1}{2e_q} e^{i(q_z z - e_q t)} \left[iq_z \left(\tilde{J}_{K+1} - \tilde{J}_{K-1} \right), q_z \left(\tilde{J}_{K+1} + \tilde{J}_{K-1} \right), 2q_T \tilde{J}_K \right] \quad \text{TM-mode}$$

$$\boldsymbol{A}_K^{(2)} = \frac{1}{2} e^{i(q_z z - e_q t)} \left[i \left(\tilde{J}_{K+1} + \tilde{J}_{K-1} \right), \left(\tilde{J}_{K+1} - \tilde{J}_{K-1} \right), 0 \right], \quad \text{TE-mode}$$

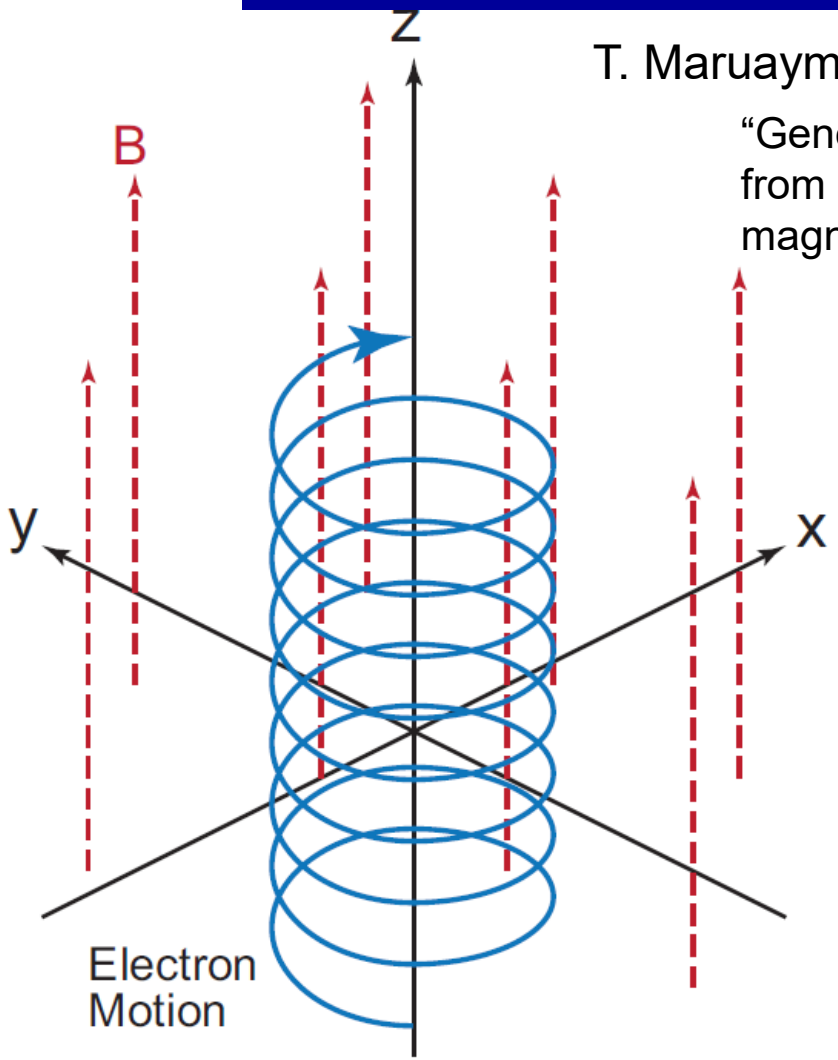
$$\tilde{J}_M(\boldsymbol{r}_T) = J_M(\sqrt{eB} q_T r_T) e^{iM\phi}.$$

Astrophysical sites with strong magnetic fields



Strong magnetic fields: 10^{12}～10^{15}G

Synchrotron radiation from electrons under a uniform magnetic field

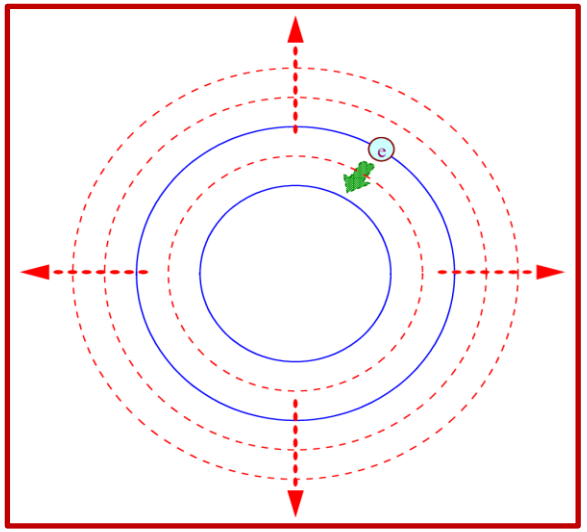


Electrons under magnetic fields are under quantization

T. Maruayma et al. Phys. Lett. B, 826, 136779 (2022).

"Generation of photon vortex by synchrotron radiation from electrons in Landau states under astrophysical magnetic fields"

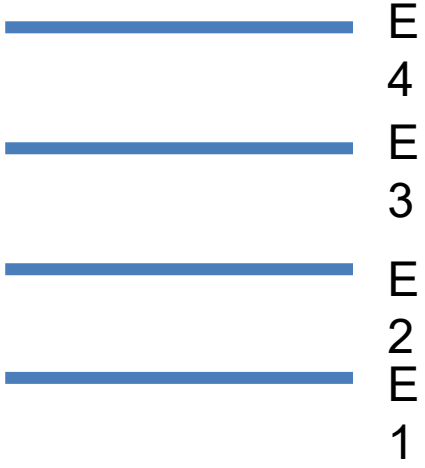
In xy-plain



When a magnetic field is weak, classical EM theory is a good approximation.

Landau quantization

Electron orbitals under a magnetic field



Here, natural unit ć=h=1

Landau energy for each eigen-state

$$E = \sqrt{2eBN_L + p_z^2 + m_e^2},$$

B: Magnetic field
Pz: z-component of momentum
e: Elementally charge
me: Mass
NL: Landau Number

Landau quantum number

$$N_L = (L + |L|)/2 + n$$

$N_L = n + L$ (when $L \geq 0$), $N_L = n$ (when $L < 0$)

$L \leq -1$ is impossible in Classical Theory

L: z-component of orbital angular momentum
n: number of nodes in Laguerre Polynomial

Wave-function of electrons

Electron wave-function can be obtained from Dirac equation.

$$\{\boldsymbol{\alpha}\cdot(-i\boldsymbol{\nabla}_r + e\boldsymbol{A}) + \beta m_e - E\}\,\psi(\boldsymbol{r}) = 0$$

Vector potential $\boldsymbol{A} = (-y, x, 0)B/2$ Symmetry gauge

Magnetic field ***B*** = *(0, 0, B)*

$$\boldsymbol{r} = (\boldsymbol{r}_T, z) = (r_T\cos\phi, r_T\sin\phi, z)$$

$$\psi(\boldsymbol{r}) = \left\{\frac{1+\Sigma_z}{2}G^{n'}_{L-1}\left(\sqrt{\frac{eB}{2}}\boldsymbol{r}_T\right) + \frac{1-\Sigma_z}{2}G^{n}_{L}\left(\sqrt{\frac{eB}{2}}\boldsymbol{r}_T\right)\right\}$$

$$\times\frac{E+m_e}{2\sqrt{R_z E}}\begin{bmatrix}\chi_s\\ \frac{\tilde{\boldsymbol{p}}\cdot\boldsymbol{\sigma}}{E+m_e}\chi_s,\end{bmatrix}e^{ip_z z},$$

σ: Pauli Matrix

Xs: Pauli spinor

$$G^n_L(\boldsymbol{r}_T) = \sqrt{\frac{n!}{\pi(n+|L|)!}}e^{iL\phi}\sqrt{eB}r_T^{|L|}e^{-r^2/2}\mathcal{L}_n^{|L|}(r_T^2)e^{iL\phi},$$

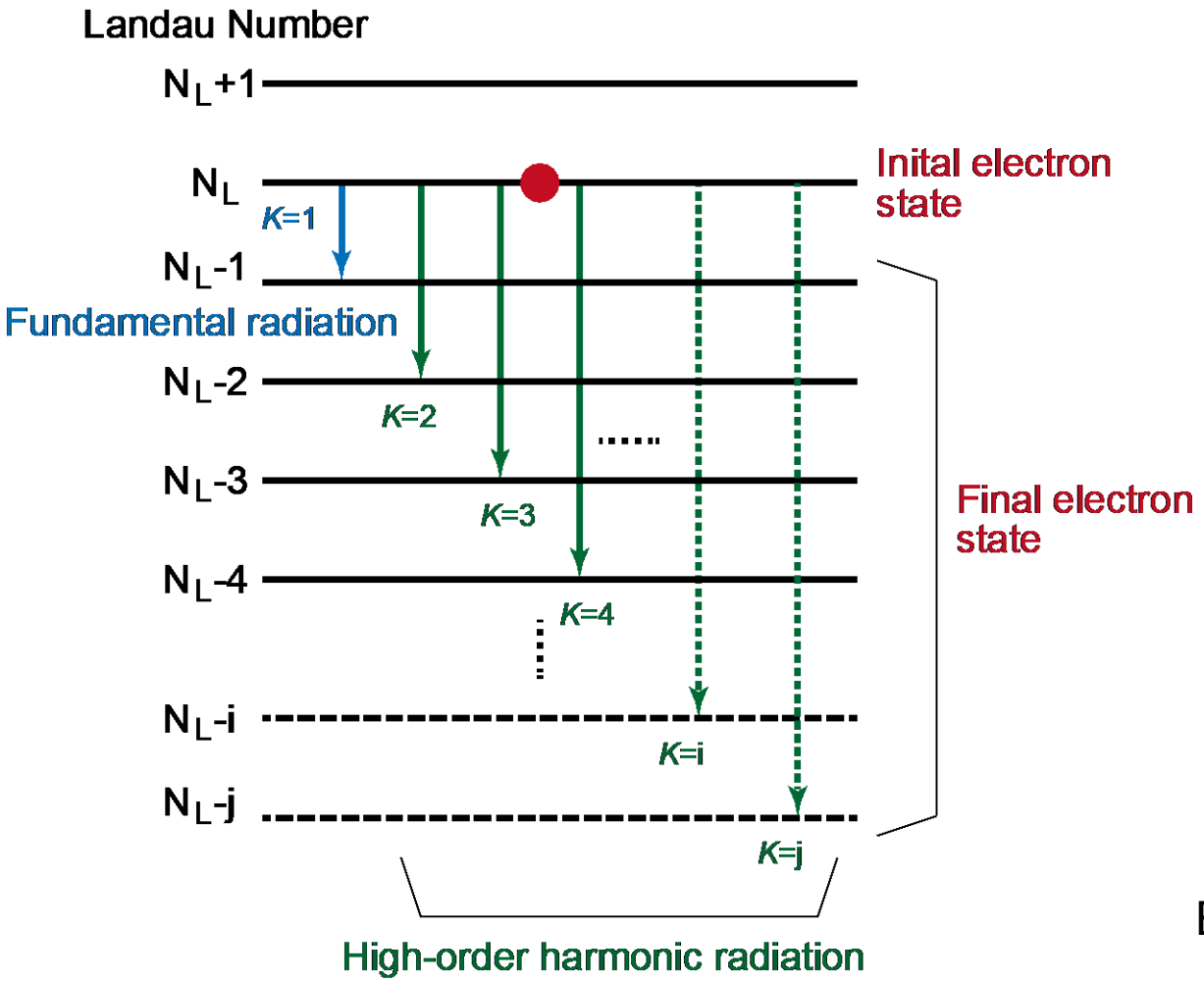
Laguerre functions

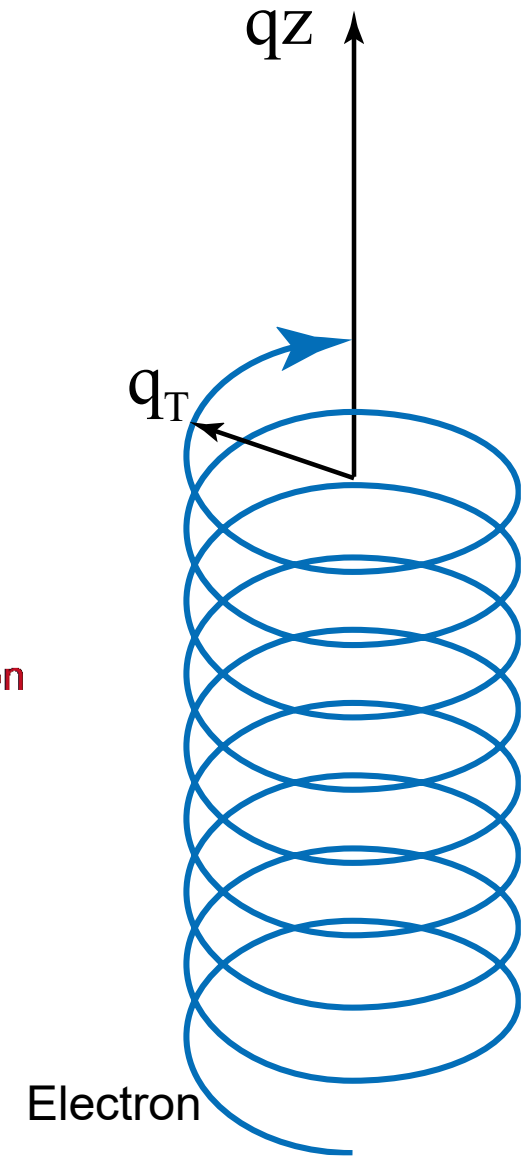
$$\tilde{\boldsymbol{p}} = (0, \sqrt{2eBN_L}, p_z),$$

High-order harmonic radiation

$|q_z| \gg q_T \Rightarrow$ Bessel wave : Photon vortex

$|q_z| \ll q_T \Rightarrow$ Cylindrical Wave : Not vortex





Decay width

Electron wave-function

Decay width

$$\Gamma_e(i) = -2\int d\boldsymbol{r}_1 d\boldsymbol{r}_2 \overline{\psi}_i(\boldsymbol{r}_1)\mathrm{Im}\Sigma(\boldsymbol{r}_1,\boldsymbol{r}_2,E_i)\psi_i(\boldsymbol{r}_2)$$

Imaginary part of self-energy of electron

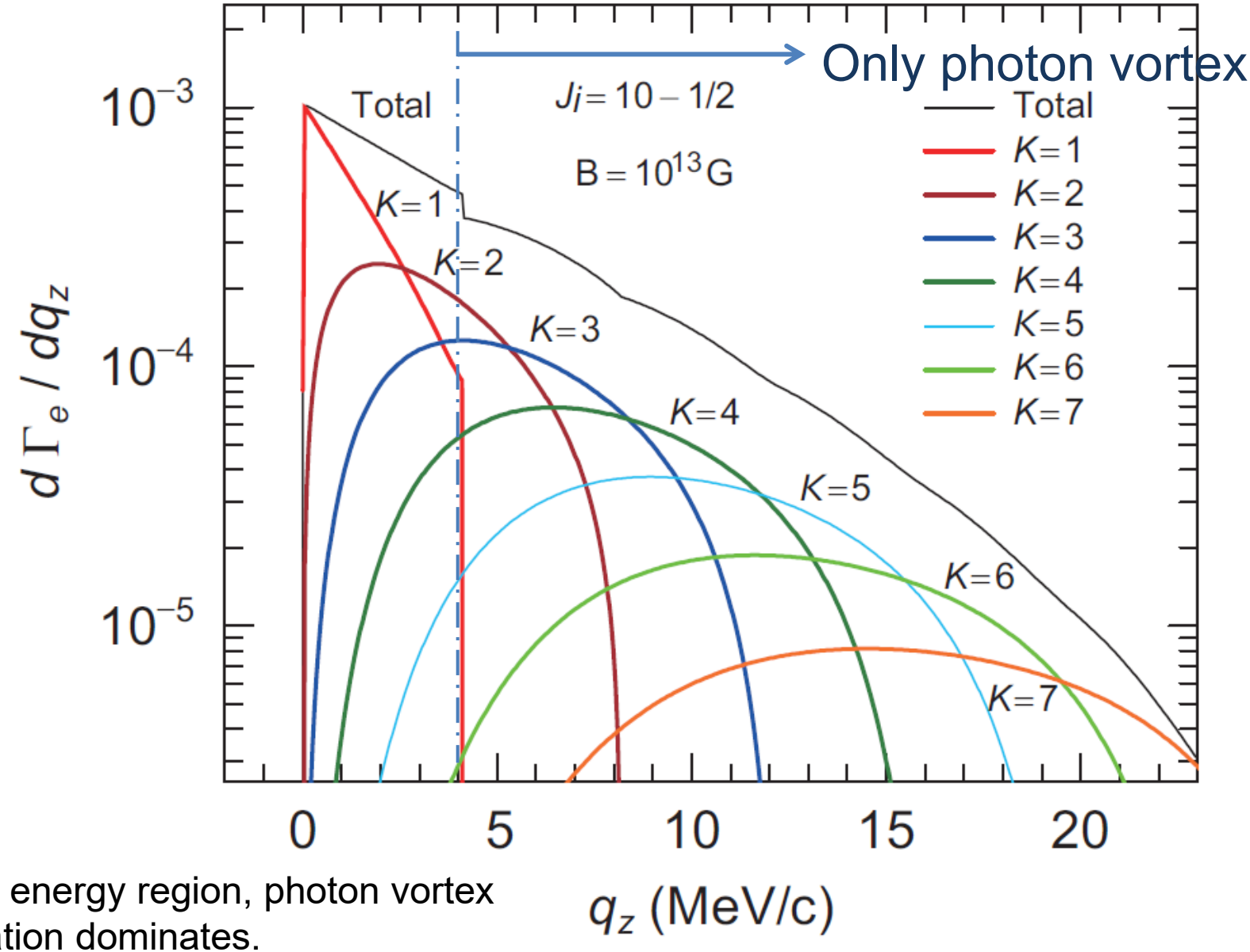
$$= \frac{e^2}{8\pi^2}\sum_{f,K,\alpha}\int \frac{dq_z dq_T q_T}{e_q}\frac{dp_{fz}}{2\pi}\delta(E_i - E_f - e_q)\left|\int d\boldsymbol{r}\overline{\psi}_f(\boldsymbol{r})A_K^{(\alpha)*}(\boldsymbol{r})\psi_i(\boldsymbol{r})\right|^2$$

$$\frac{d\Gamma_{if}^{(a)}}{dp_{fz}} = \frac{d\Gamma_{if}^{(a)}}{dq_z} = \frac{e^2}{8\pi^2}\left|\int d\boldsymbol{r}_T\overline{\phi}_f(\boldsymbol{r}_T)V_K^{(\alpha)*}(\boldsymbol{r}_T)\phi_i(\boldsymbol{r}_T)\right|^2$$

$$\psi_b(\boldsymbol{r}) = \frac{1}{\sqrt{R_z}}\phi_b(\boldsymbol{r}_T)e^{ip_{bz}z}$$ Electron wave-function.

$$A_K^{(\alpha)}(\boldsymbol{r}) = V_K^{(\alpha)}(\boldsymbol{r}_T)e^{iq_z z}$$ Photon Wave-function

Energy spectrum



In high energy region, photon vortex generation dominates.

Circular polarization

State-1

$$\boldsymbol{A}(h=+1)-\boldsymbol{A}(h=-1)$$

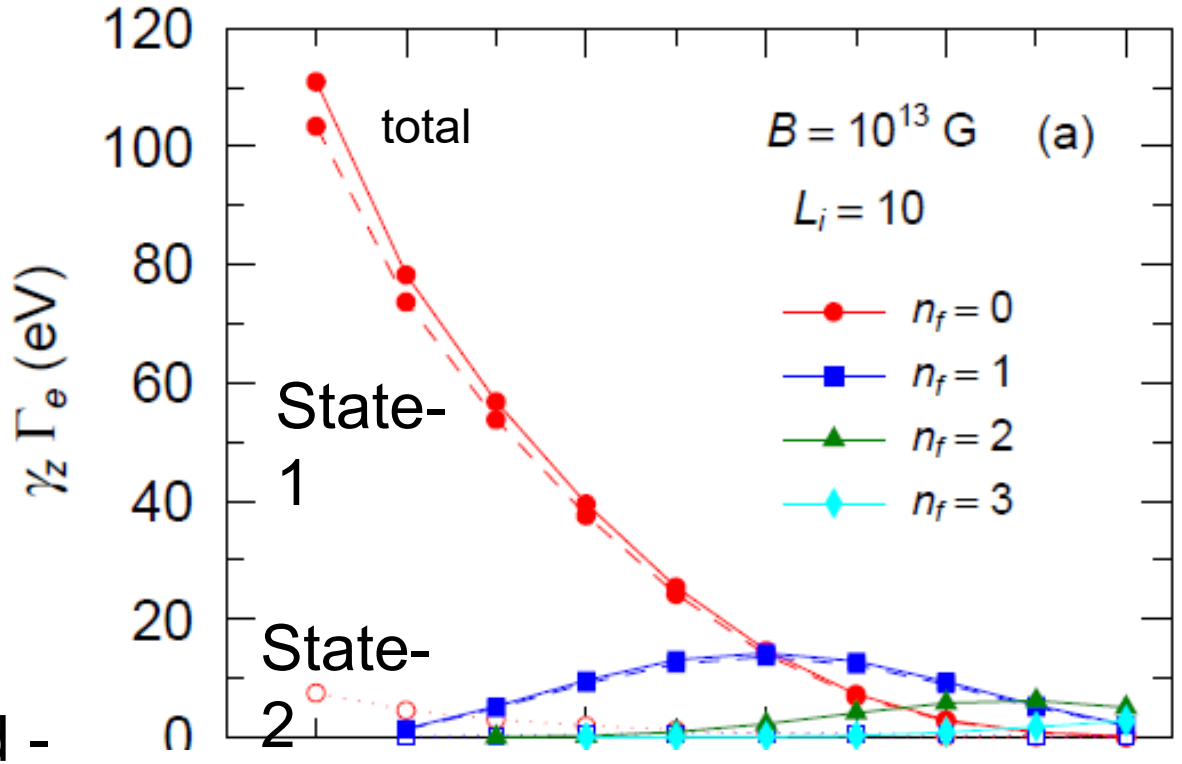
$$\boldsymbol{A}(h=+1)+\boldsymbol{A}(h=-1)$$

State-2

State-1 dominates in most cases

Photon with h + -1 and -1 are mixed.

Degree of circular polarization is low !



Nature of photon vortex

This is because the vector of photon propagation differ from the motion of photon.

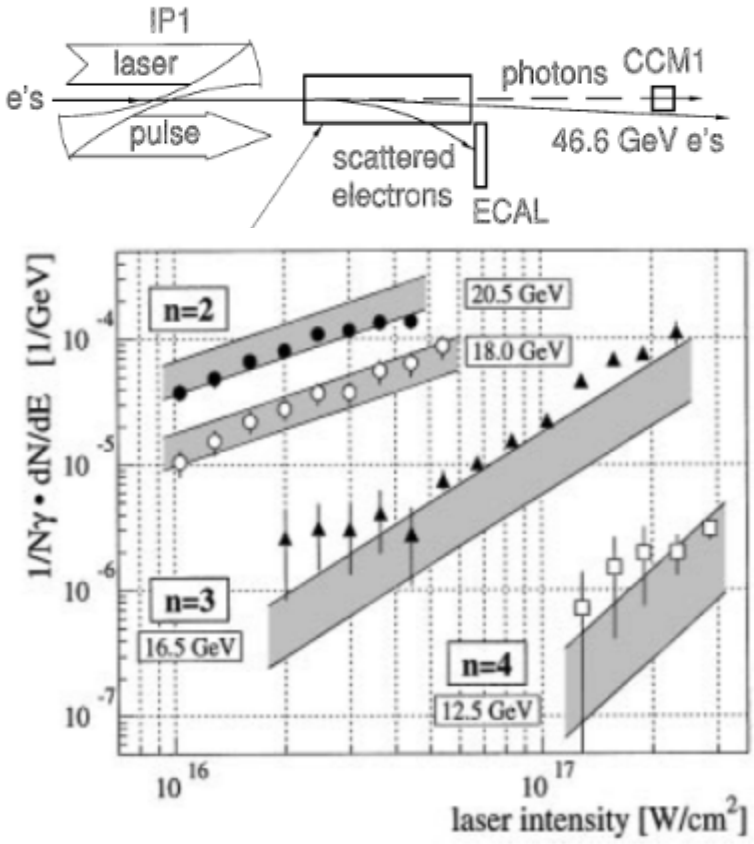
Nonlinear inverse Compton scattering

Bula et al., Phys. Rev. Lett. (1996)

a0=0.84, Ee=12.5-20.5GeV

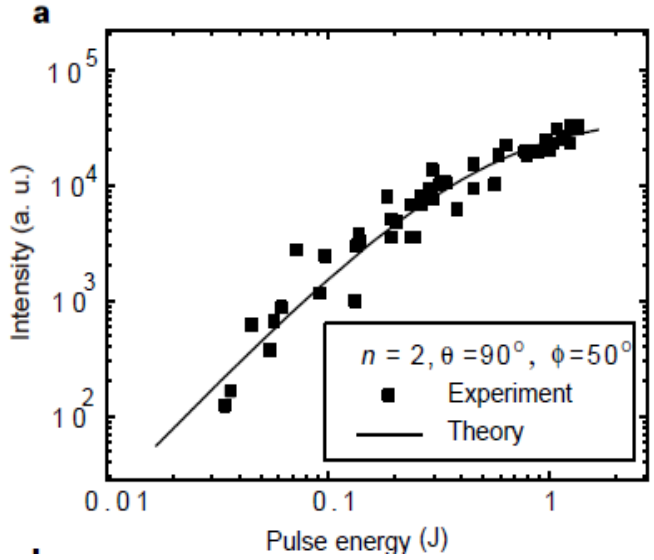
$$E_{n\omega} \approx \frac{4\gamma^2 n\hbar\omega_L}{1 + a_0^2/2 + \gamma^2\Theta^2}$$

$$a_0 = \frac{eE}{mc\omega} = 0.855\lambda\ [\mu\mathrm{m}] \times 10^{-9}\sqrt{I[\mathrm{W/cm^2}]}$$



Normalized scattered electron yields

1.055 μm、4TW

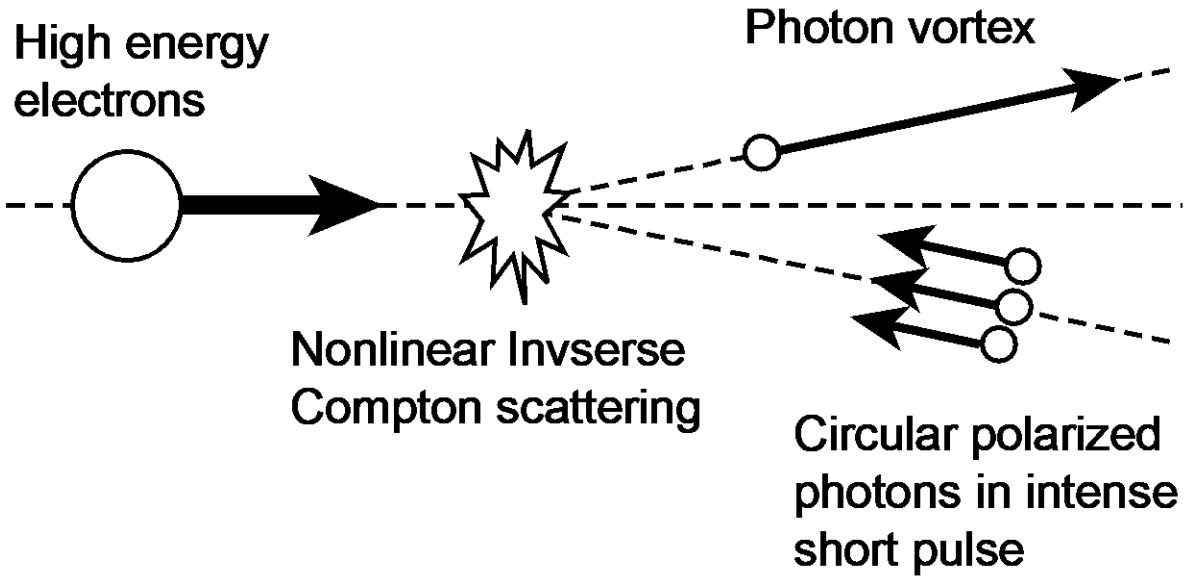


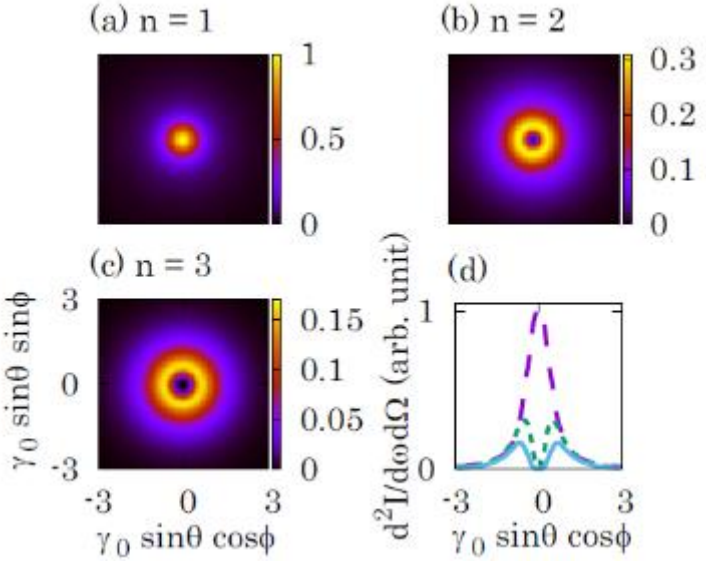
S. Chen, et al. Nature, 396, 653 (1998).

Nonlinear inverse Compton scattering with circularly polarized laser

Y. Taira, T. Hayakawa, M. Katoh, Scientific Reports, 7, 5018 (2017).

Proposal of photon vortex generation by non-linear inverse Compton scattering with circularly polarized intense laser pulse





The spins of multi photons is converted to the angular momentum of a single photon by nonlinear Compton scattering.

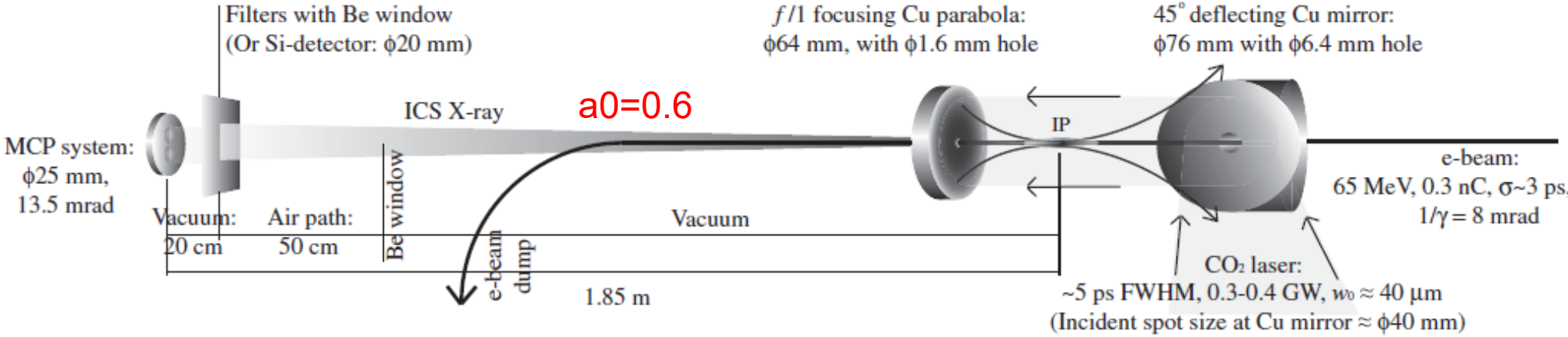
Previous experiment

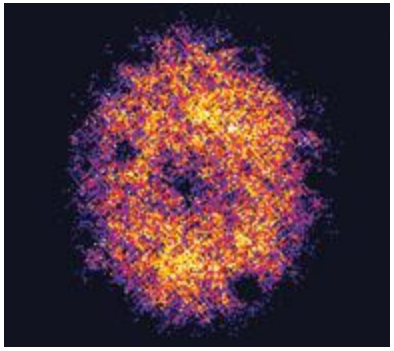
Observation of red shifting and harmonic radiation in inverse Compton scattering

Y. Sakai, et al. Phys. Rev. STAB, 18, 060702 (2015)　BNL ATF

Circularly polarized High Power CO_2 laser

Ee = 65 MeV

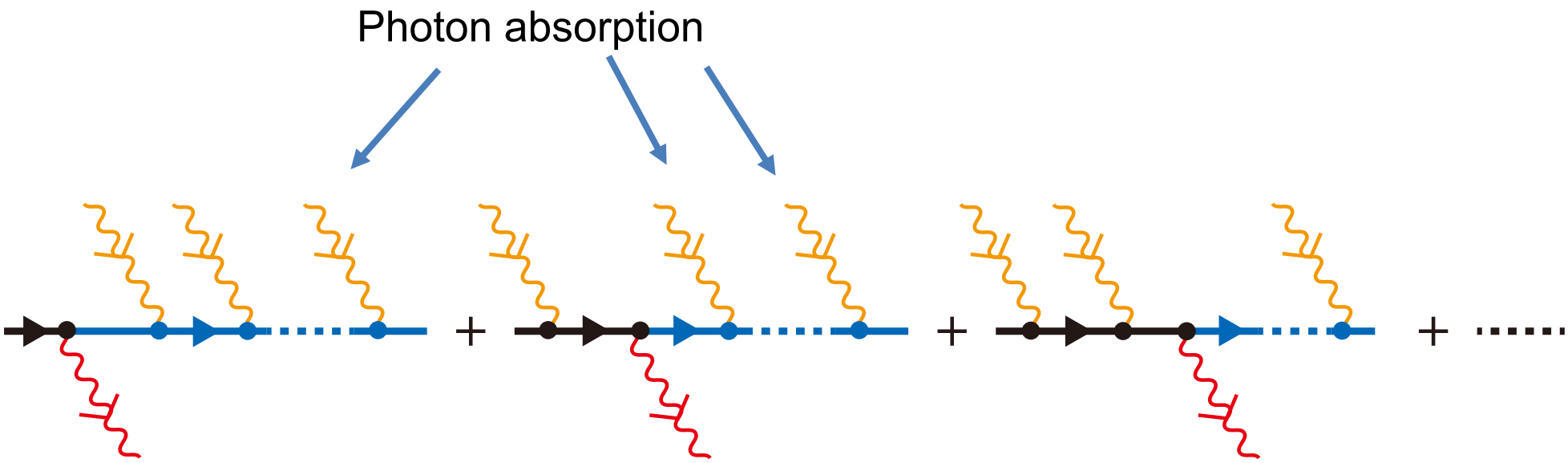




Observation of 2nd harmonics

Circle structure ← Feature of optical vortex

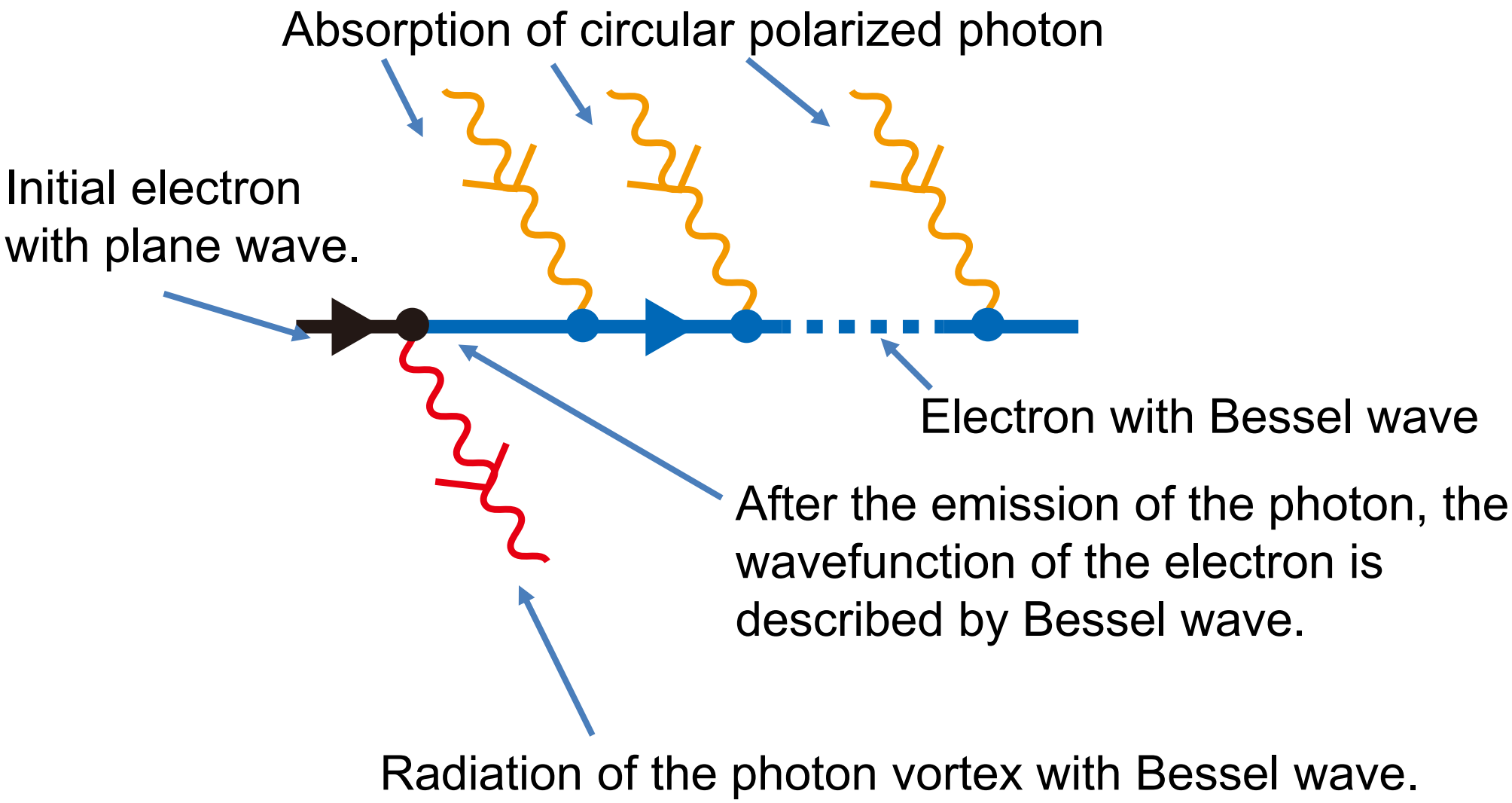
Feynman diagram



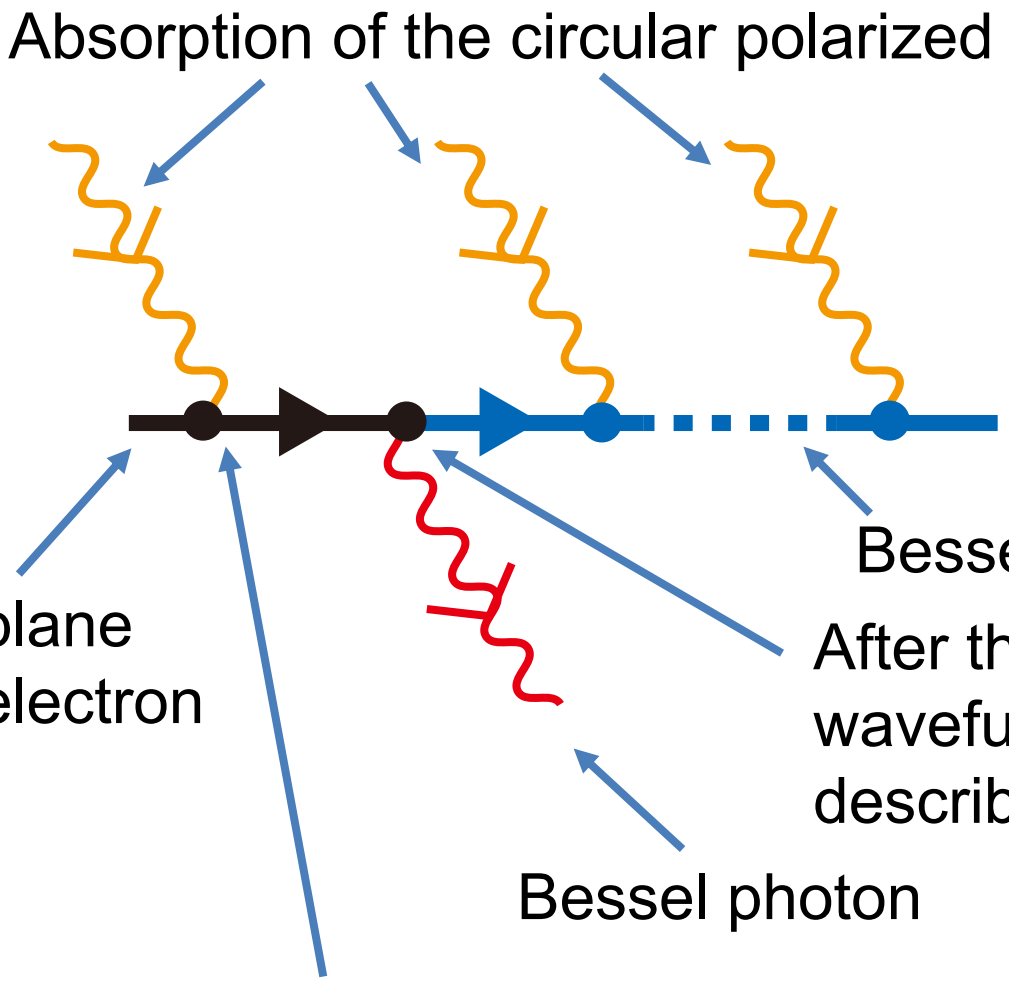
First, a photon is emitted and next the other photons are absorbed by the electron.

A photon is absorbed, a photon is emitted, and the other photons are absorbed.

Absorption after radiation

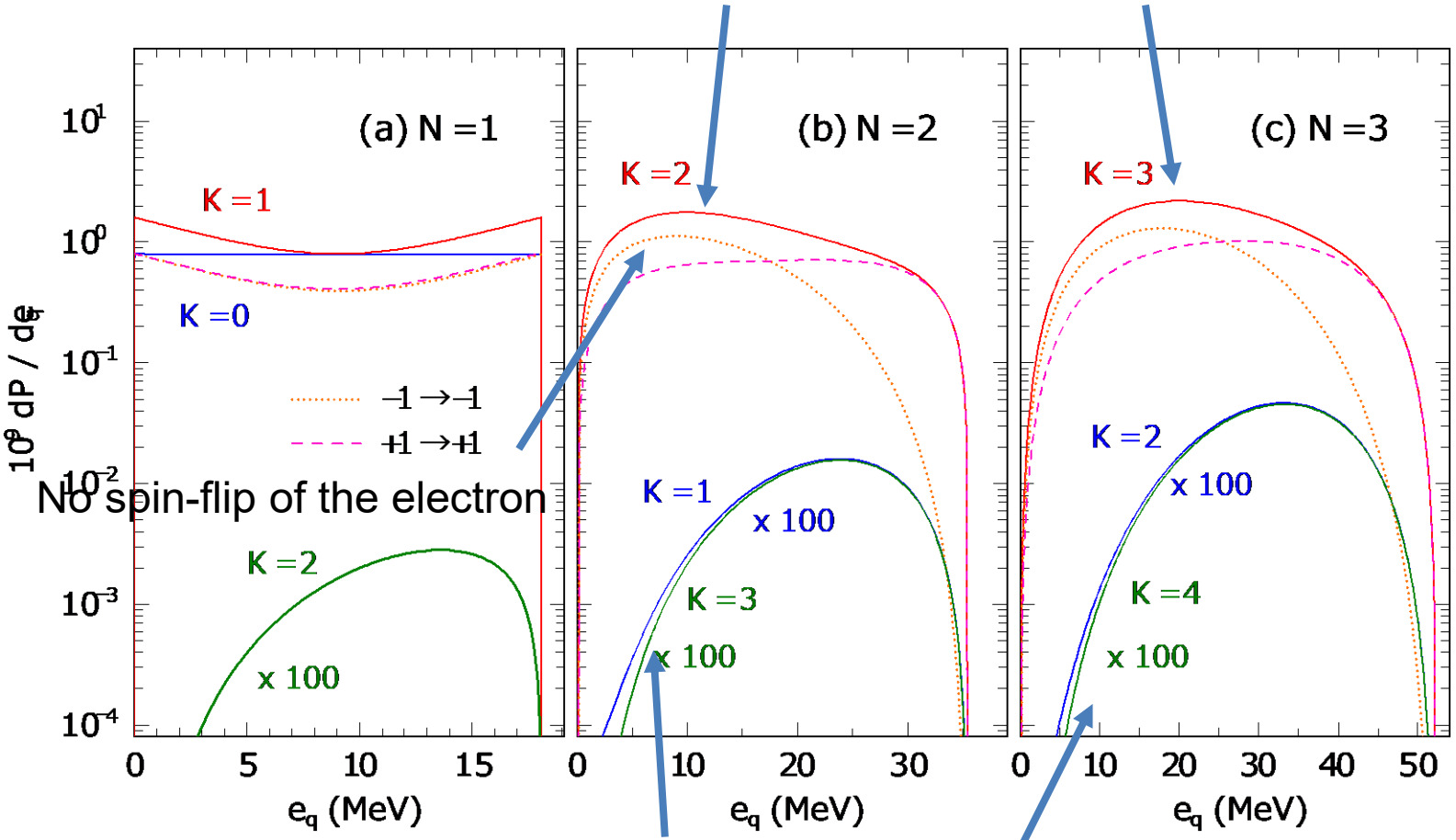


Photon emission after one photon absorption

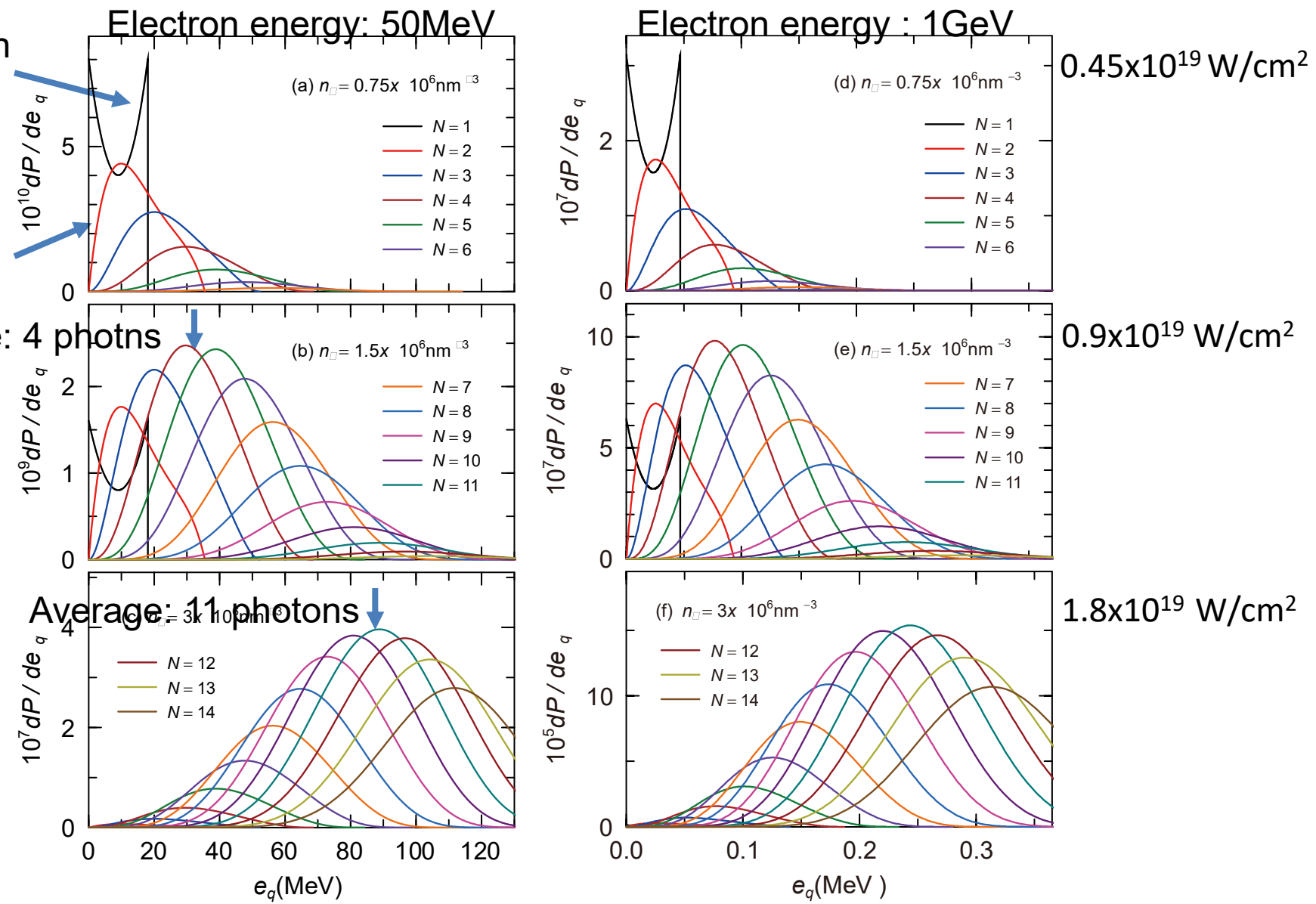


zTAM of the radiated photon vortex

When N photons are absorbed, a photon vortex with K=N is predominantly radiated.

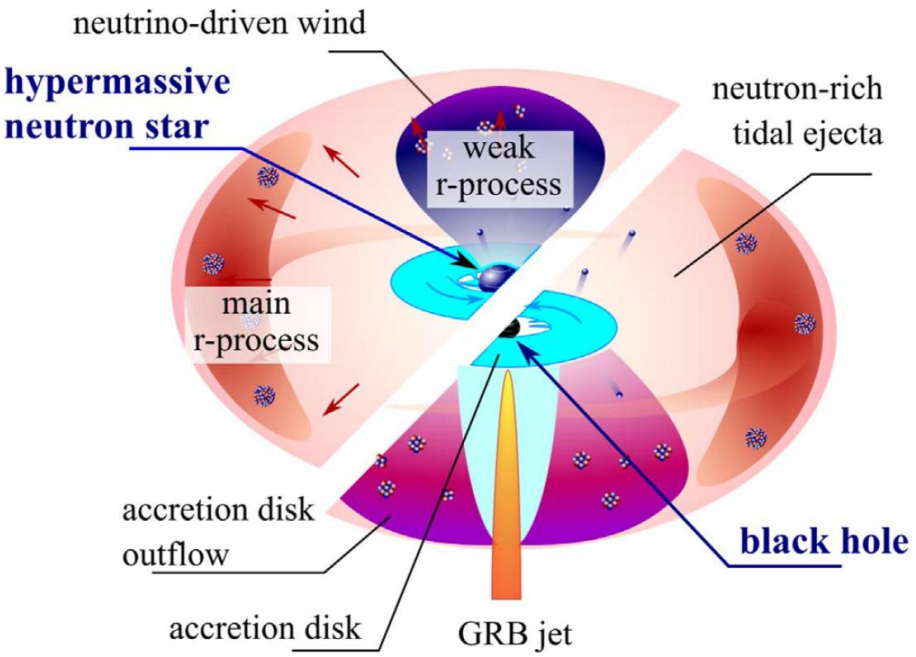


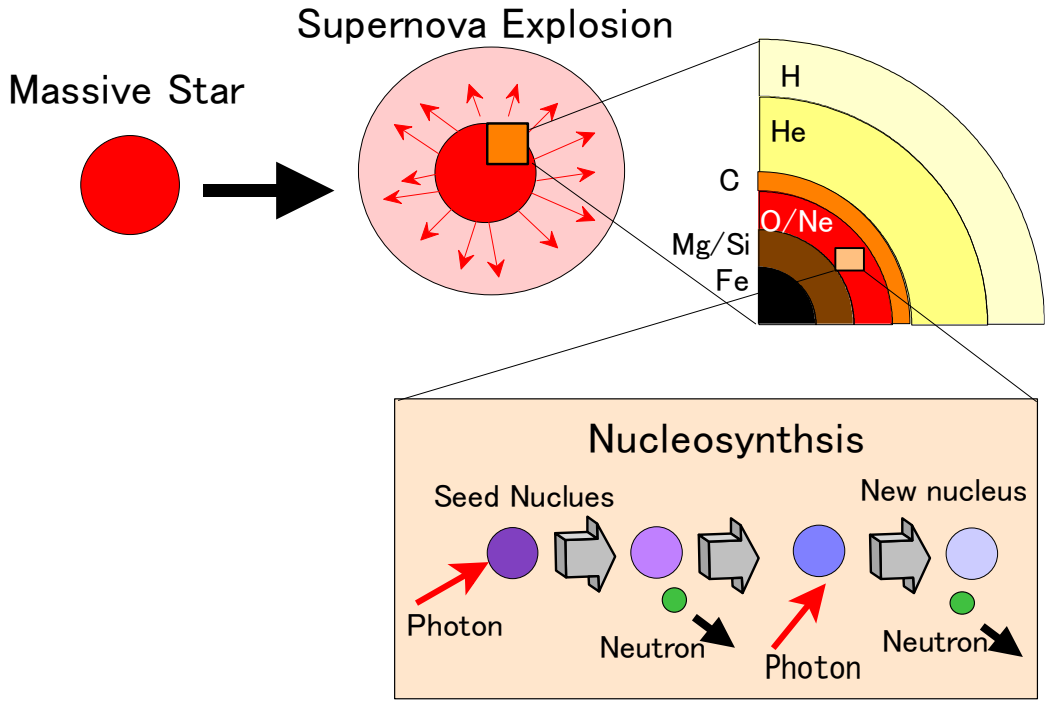
Energy spectra



Possible effect on stellar nucleosynthesis

O. Korobkin, Astrophysical J. 910, 116 (2021).



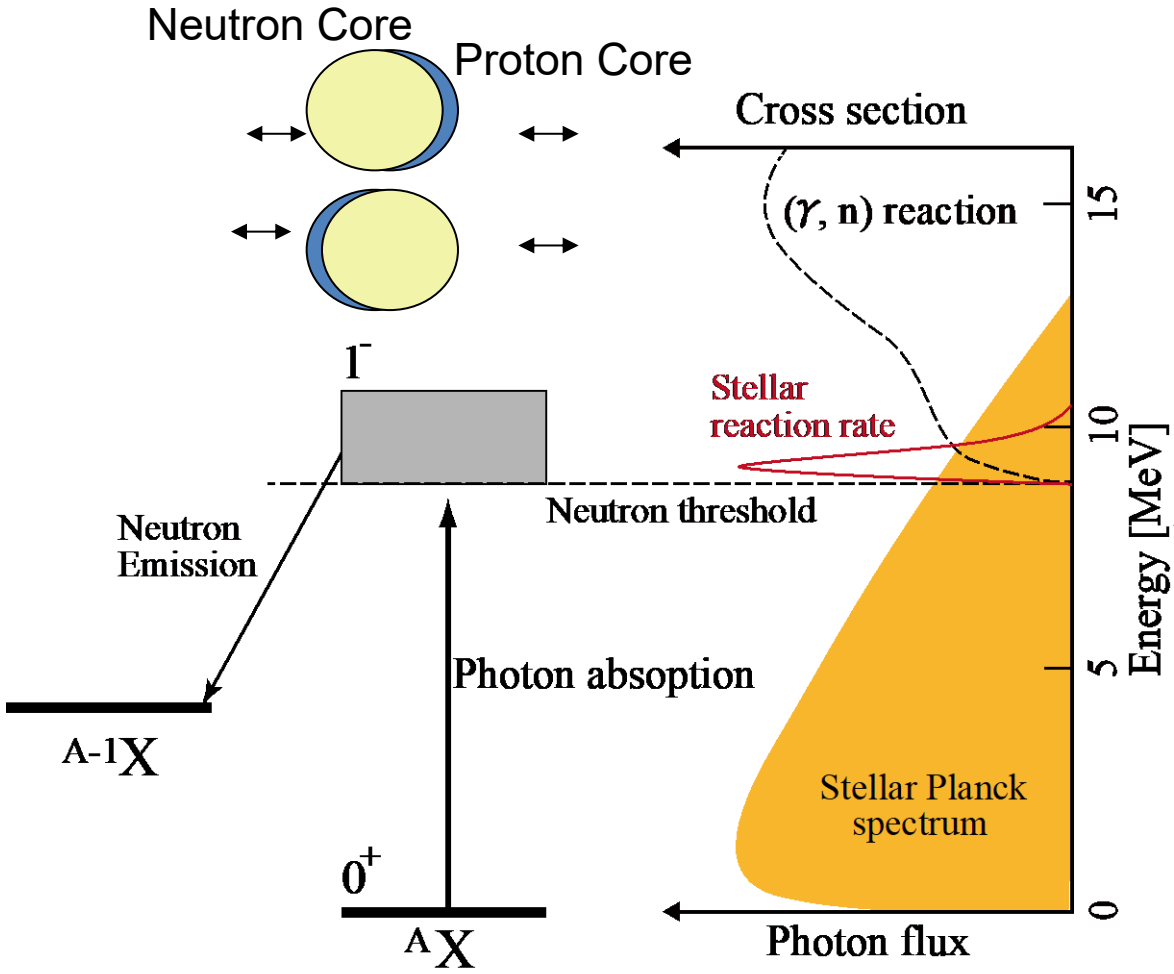


When the r-process inner region in Black Hole forming with strong magnetic fields occurs, photonuclear reaction rate may decrease and the r-process path may shift to neutron rich region.

Gamma-process in MHD supernova

Production of p-nuclei may decrease.

“photon vortex” on nuclear reactions



Conservation law of angular momentum

$$|\ Ji-Jp\ | \leq Jf \leq |Ji+Jp\ |$$

When the total angular momentum of an incident photon is higher than 1, GDR on even-even nucleus with J=0 is forbidden.

Y. Taira, T. Hayakawa, M. Katoh, Scientific Reports, 7, 5018 (2017).

Photodisintegration reactions with photon vortex

Andrei Afanasev, et al. J. Phys. G 45, 055102 (2017).

$$\gamma + d \rightarrow n + p$$

$$|J_i - J_f| \leq |j| \leq J_i + J_f;$$
$$M_f - M_i = \lambda$$

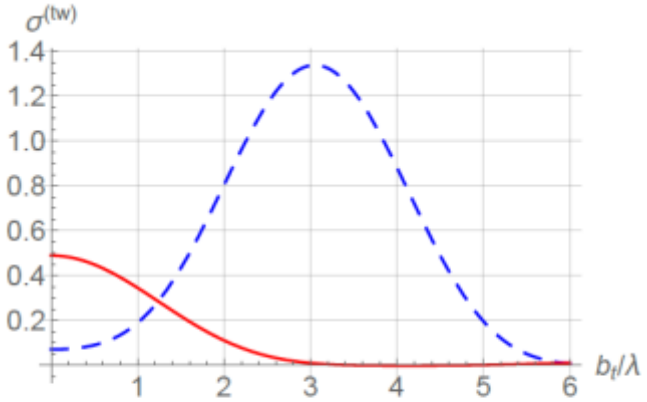


FIG. 4: Total cross section in arbitrary units, as a function of the position of the target center b_t for the ${}^3S_1 \rightarrow {}^1S_0$ process, excited by twisted photon beam. Dashed-blue line corresponds to ($m_\gamma = 0, \lambda = 1$), and solid-red line to ($m_\gamma = 0, \lambda = 1$). Pitch angle is $\theta_k = 0.1$ rad.

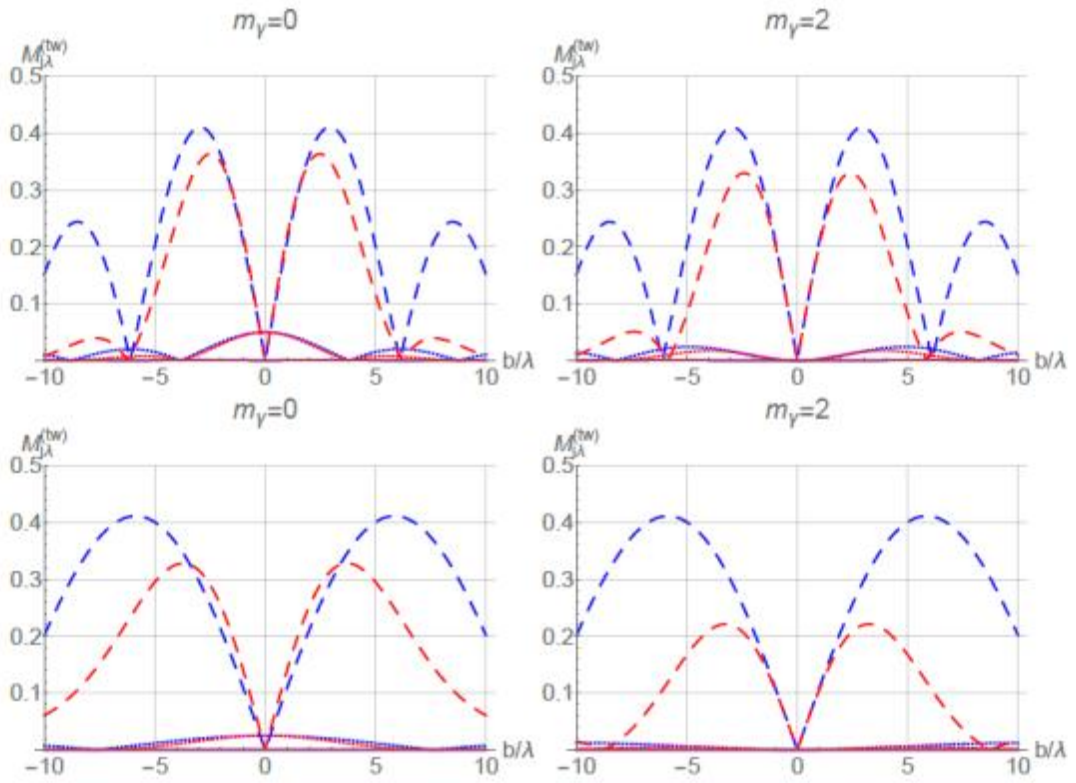
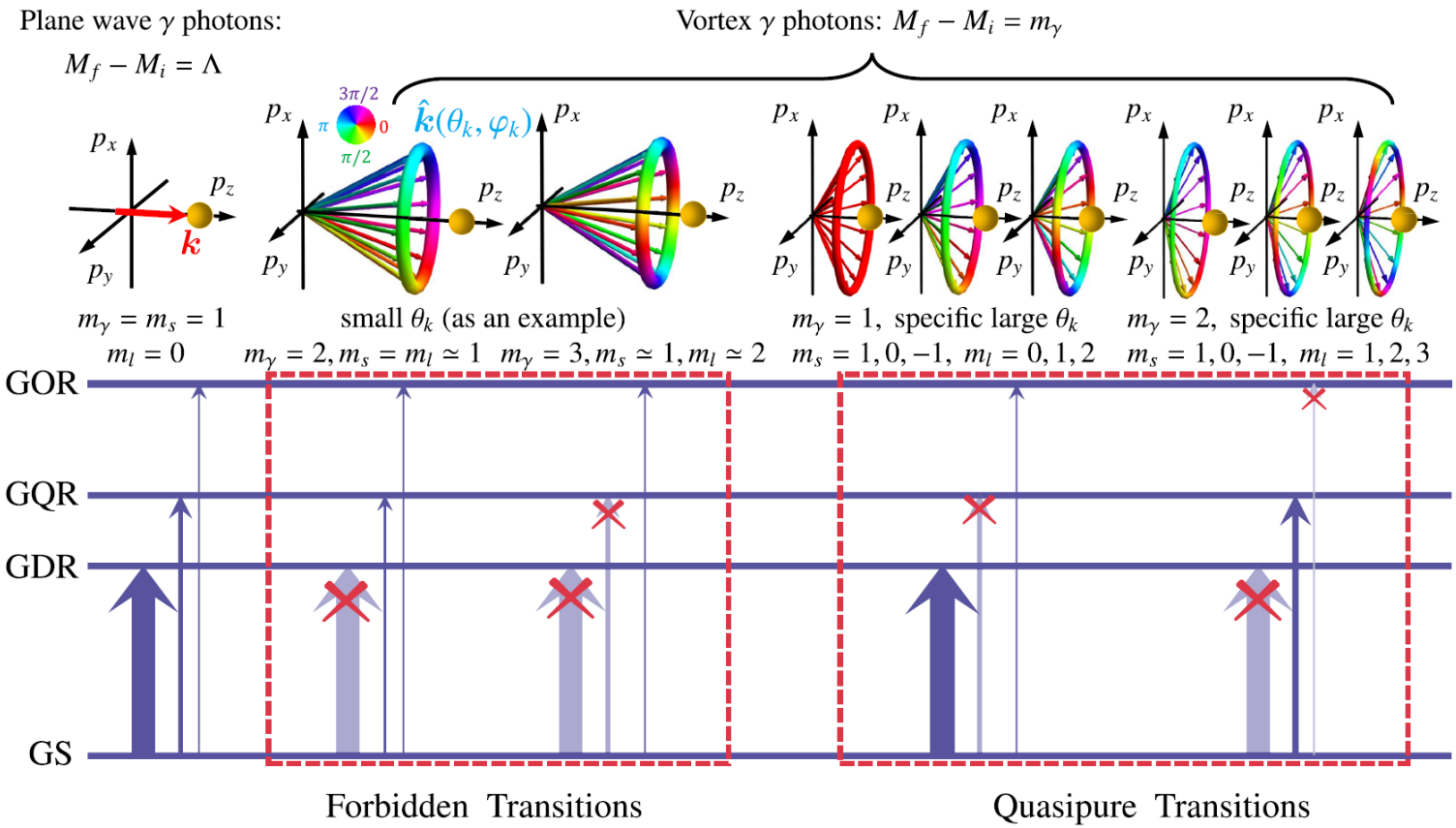


FIG. 3: Relative photo-absorption amplitudes $M^{(tw)}_{j\lambda}$ for $M1 \rightarrow {}^1S_0$ transition for BB (blue), Eq. (50); and for BG (red), Eq. (53) as functions of the impact parameter scaled with the photon wavelength. The pith angles considered are $\theta_k = 0.1$ rad - top row; $\theta_k = 0.05$ rad - bottom row; and waist $w_0/\lambda = 6.0$. Dashed lines correspond to the case $M_f - M_i = 1$, dotted lines to $M_f - M_i = 0$, and solid lines to $M_f - M_i = -1$.

2.2 MeV gamma-vortex is required.

Interaction between Photon vortex and Nuclei

Zhi-Wei Lu, et al. Physical Review Letters 131, 202502 (2023)



The calculation using the fully self-consistent random-phase approximation plus particle-vibration coupling model based on Skyrme density functional.

Effects on stellar nucleosynthesis

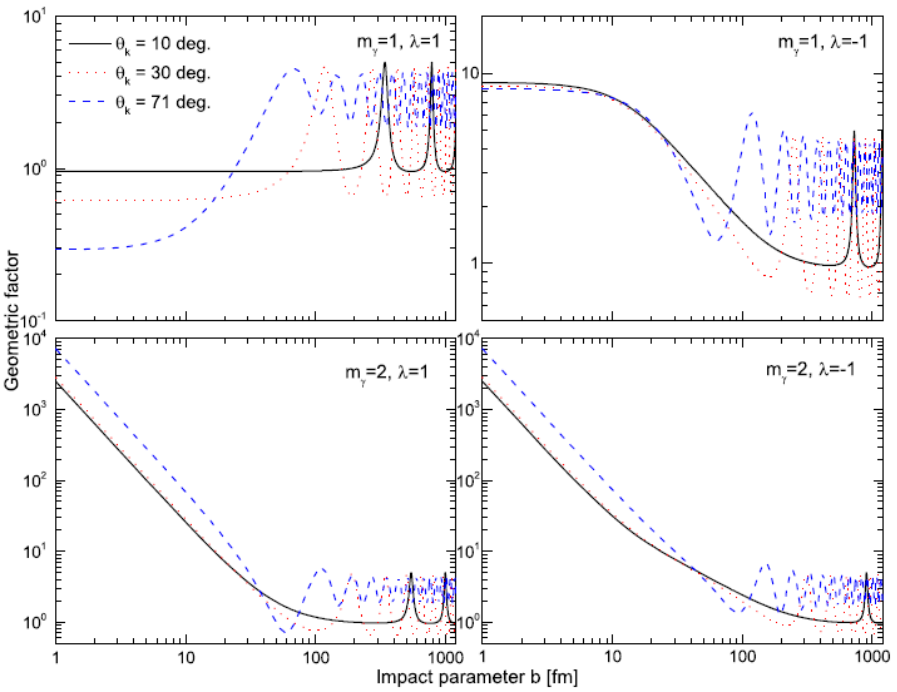
The ratio of the high-K photon vortex to the fundamental photon at a fixed impact parameter b.

$$\sigma_{abs}^{vo} = \sum_{X=el}^{mag} \sum_{L=1}^{\infty} \frac{\sigma^{XL}}{\cos\theta_k} \frac{\sum_{M=-L}^{L} |d_{M\lambda}^{L}(\theta_k) J_{m_\gamma - M}(\kappa b)|^2}{\sum_{\sigma=-1}^{1} |d_{\sigma\lambda}^{1}(\theta_k) J_{m_\gamma - \sigma}(\kappa b)|^2},$$

The Hauser-Feshbach model

The ratio of the gamma-ray and neutron at specific angles.

Yi Xu, et al. Phys. Lett. B 852 (2024) 138622



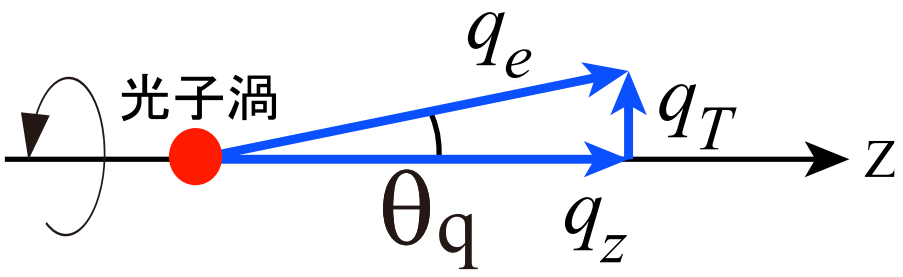
GQR is enhanced inside of b= 100 fm.

The cross section inside 1000 fm was integrated.

Calculation for 137 nuclides.

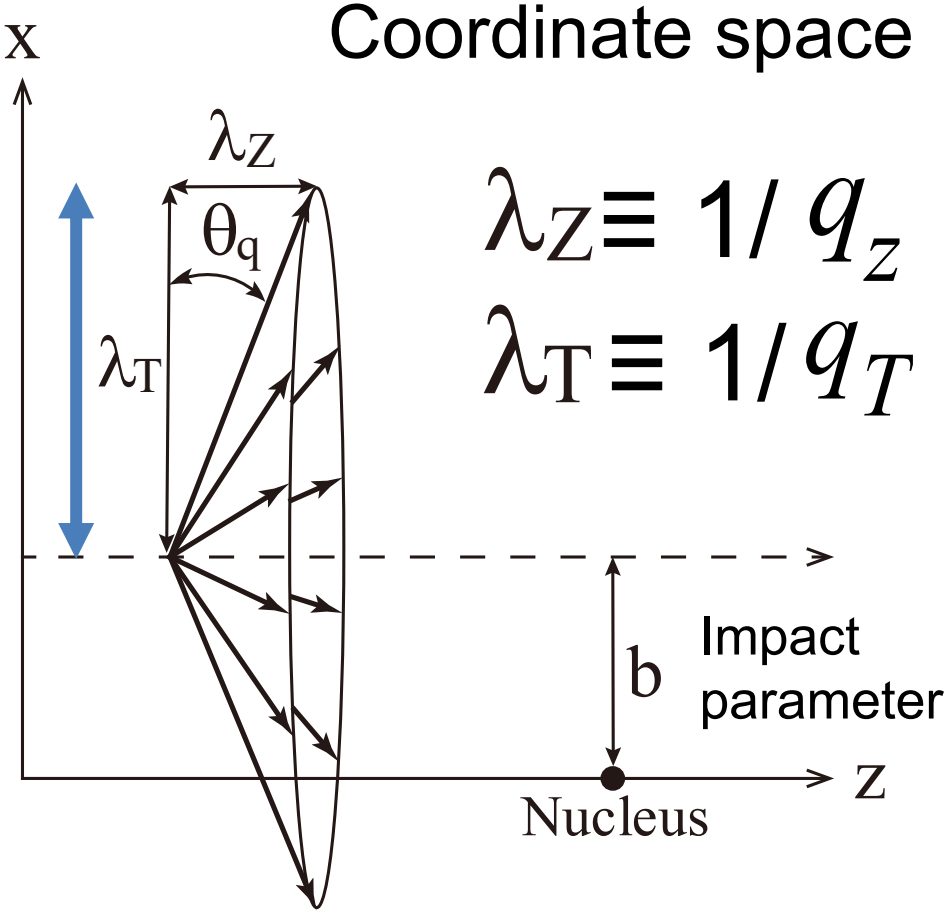
Photon vortex in coordinate space

Momentum space



The effect of vortex increases with increasing θ_q

Coordinate space



$\lambda_Z \equiv 1/q_z$

$\lambda_T \equiv 1/q_T$

λ_T : Size of photon vortex

Transition Strength with Bessel Wave

Photon Wave Func. Bessel Wave

$$\boldsymbol{A}_K^h(\boldsymbol{r}) = e^{iq_z z}\left[\frac{i(e_q + hq_z)}{2e_q}\tilde{J}_{K-1}\boldsymbol{e}_+ + \frac{i(e_q - hq_z)}{2e_q}\tilde{J}_{K+1}\boldsymbol{e}_{-1} + \frac{hq_T}{\sqrt{2}e_q}\tilde{J}_K\boldsymbol{e}_0\right]$$

$$\tilde{J}_M(q_T\boldsymbol{r}_T) = J_M(q_T r_T)e^{iM\phi}$$

Fourier Transformation

$$\boldsymbol{A}_K^h(\boldsymbol{p}) = \int d^3r e^{-i\mathbf{p}\cdot\mathbf{r}}\boldsymbol{A}_K^h(\boldsymbol{r}) = \frac{(2\pi)^2}{q_T}\delta(p_z - q_z)\delta(p_T - q_T)(-i)^{K-h}e^{i(K-h)\phi_p}\boldsymbol{e}(\boldsymbol{p},h)$$

$$\boldsymbol{e}(\boldsymbol{p},h) = \frac{(1 + h\cos\theta_p)}{2}e^{-i\phi_p}\boldsymbol{e}_+ + \frac{(1 - h\cos\theta_p)}{2}e^{i\phi_p}\boldsymbol{e}_- + \frac{h\sin\theta_q}{\sqrt{2}}\boldsymbol{e}_0,$$

Polarization Vector $\perp \boldsymbol{p}$

Multipole Expansion

$$\boldsymbol{e}(\boldsymbol{p},h)e^{i\mathbf{q}\cdot\mathbf{r}} = \sum_{JM,\kappa}\sqrt{2\pi(2J+1)}(i)^J\mathcal{D}^J_{M,h}(\phi_p,\theta_p,0)\boldsymbol{T}^\kappa_{JM},$$

Wigner D-Function

$$\mathcal{D}^J_{M,h}(\phi_p,\theta_p,0) = \exp(-iM\phi_p)d_{Mh}(\theta_p)$$

Excitation to Various $\boldsymbol{M}$

Wigner d-Matrix

Transition Strength with Bessel Wave 2

Shifting Central Axis of BW with b

$$\mathcal{A}^{Kh}_{JM\kappa}(b) = < J, M, \kappa | \int d^3r \hat{\boldsymbol{J}}(\boldsymbol{r}) \cdot \boldsymbol{A}^h_K(\boldsymbol{r} - \boldsymbol{b}) | 00 >$$

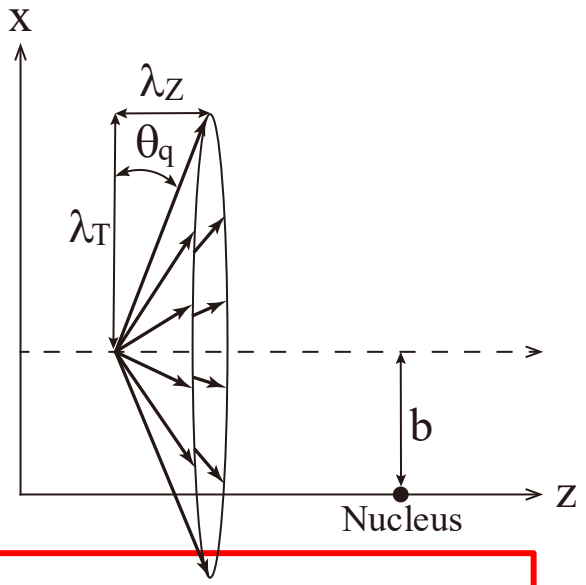
$$= \int \frac{d^3p}{(2\pi)^3} e^{-i\mathbf{p}\cdot\mathbf{b}} \frac{(2\pi)^2}{q_T} \delta(p_z - q_z)\delta(p_T - q_T)(i)^{J-K+h} e^{i(K-h-M)\phi_p}$$

$$\times \sqrt{2\pi(2J+1)} d^J_{M,h}(\theta_p) \| T^\kappa_J \|.$$

Transition Probability at fixed b

$$P^{Kh}_{JM\kappa}(b) = \left| \left\langle J, M, \kappa | \int d^3r \hat{\boldsymbol{J}}_{\rm nuc}(\boldsymbol{r}) \cdot \boldsymbol{A}^h_K(\boldsymbol{r} - \boldsymbol{b}) | 0, 0, + \right\rangle \right|^2$$

$$= 2\pi \, |d^J_{M,h}(\theta_q)|^2 [J_{M-K}(q_T b)]^2 \, \| T^\kappa_J \|^2 .$$



Ratio of BW to PW

$$R_K(b) = \sum_{M=-J}^{J} \frac{P^{Kh}_{JM\kappa}(b)}{\mathcal{P}^{(0)}_{J\kappa}} = \sum_{M=-J}^{J} |d^J_{M,h}(\theta_q)|^2 [J_{M-K}(q_T b)]^2$$

Reduces matrix element vanishes, and the ratio can be calculated without the detailed nuclear structure calculation.

Transition Strength with Bessel Wave 3

Integrating over Impact Parameters ***b***

$$\mathcal{P}^{Kh}_{JM\kappa} = \frac{1}{S_T}\int d\boldsymbol{b}\left|\int d^3r < J,M,\kappa|\hat{\boldsymbol{J}}(\boldsymbol{r})\cdot\boldsymbol{A}^h_K(\boldsymbol{r}-\boldsymbol{b})|0>\right|^2$$

S_T : Cross-Section in System

$$S_T = \frac{2\pi}{q_T}\delta(p_T - q_T)$$

Transition Probability of BW

$$\mathcal{P}^{Kh}_{JM\kappa} = 2\pi\left|d^J_{M,h}(\theta_q)\right|^2\|T^\kappa_J\|^2.$$

$$\int dr\, rJ_n(qr)J_n(pr) = \frac{1}{q}\varepsilon(p-q)$$

=1

Identical

Transition Probability of PW

$$\mathcal{P}^K_{J\kappa} = \sum_M \mathcal{P}^{Kh}_{JM\kappa} = 2\pi\|T^\kappa_J\|^2.$$

The total reaction cross sections of BW and PW are identical, and the isotopic abundances produced in the astrophysical environments are not changed.

Impact Parameter (IP) Dependence

Exc. Prob. In BW

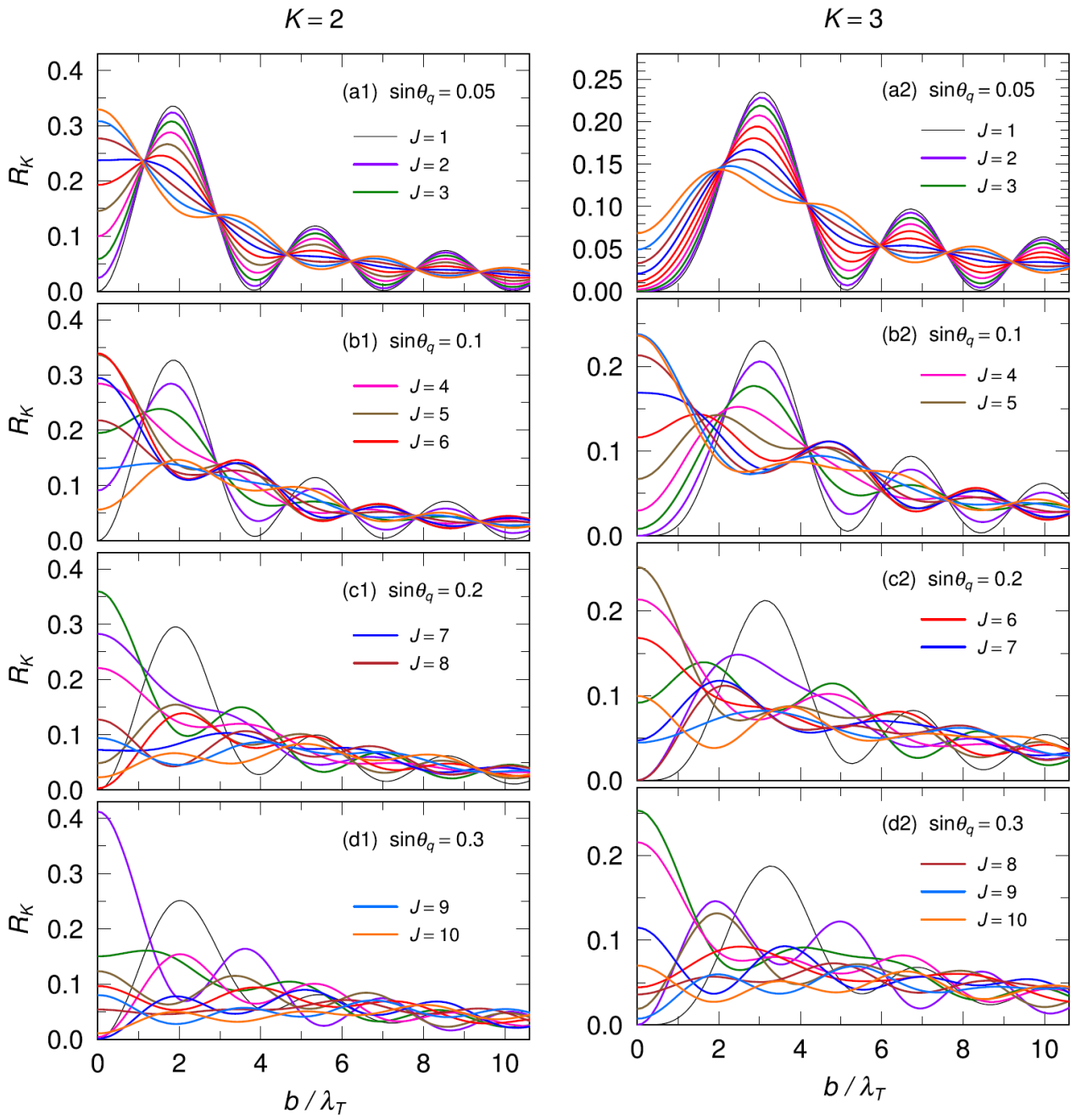
Exc. Prob. In PW

$\sin\theta_q = q_T/|\boldsymbol{q}|$

This value is fixed for BW

In small b , Contributions. from $J < K$ are small

$\lambda_T = 2\pi/q_T$



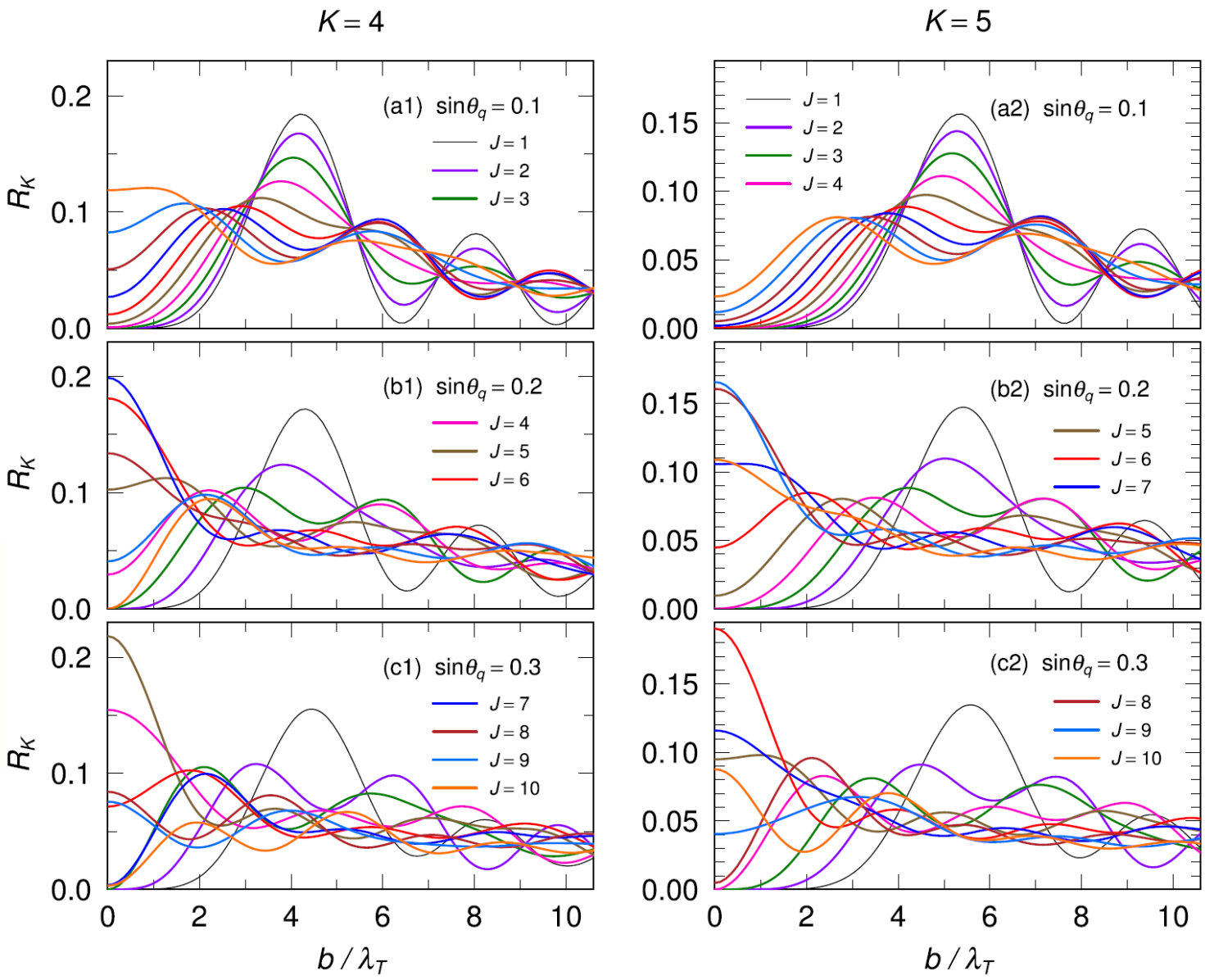
Impact Parameter (IP) Dependence

Orderly
for small θ_q

Chaos
for large θ_q

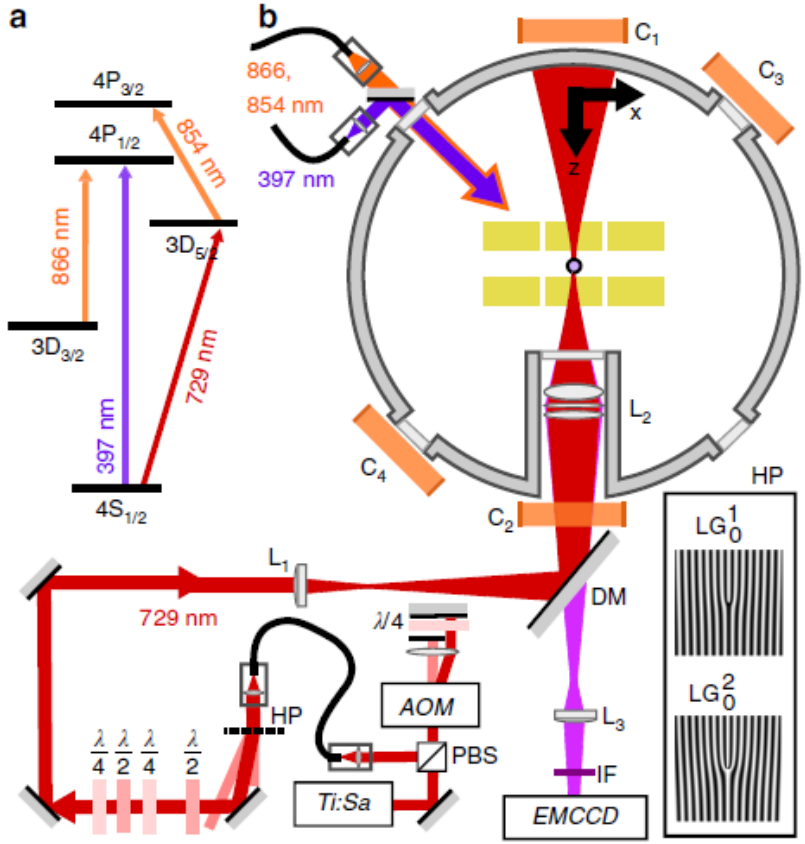
In small b ,
Contributions.
from
$J < K$ are small

$\lambda_{\mathrm{T}} = 2\pi/q_T$



Experiment on Atom (not nucleus)

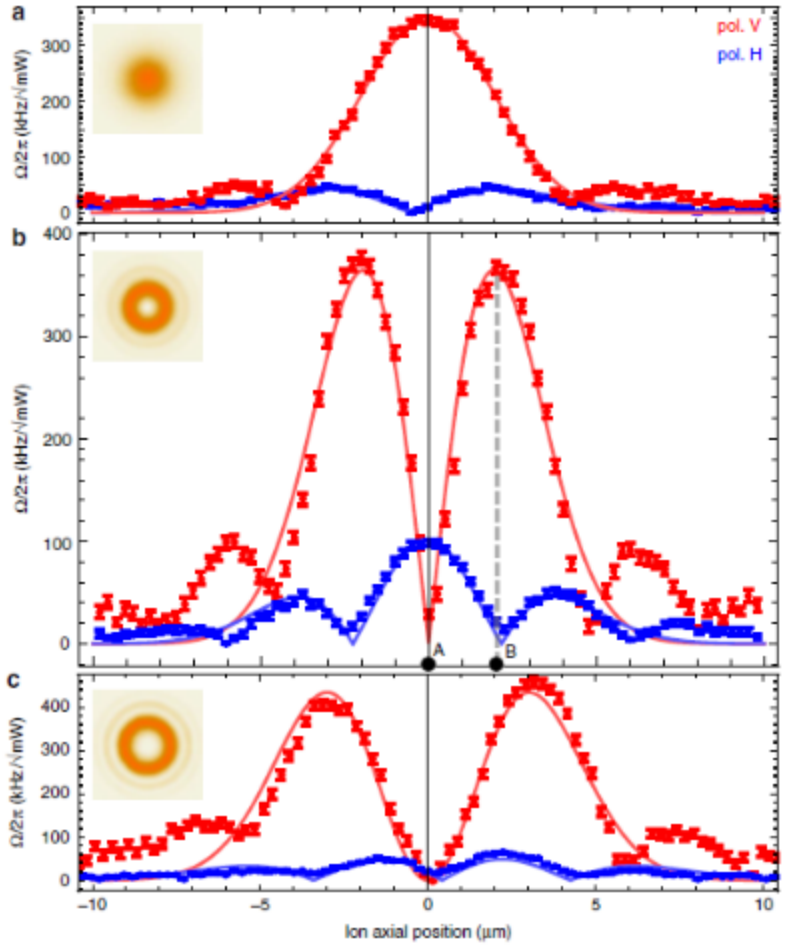
An atom is fixed by the ion trap.



GL00

GL10

GL20



Christian T. Schmiegelow, Nature Comm. 7:12998 (2016).
Transfer of optical orbital angular momentum to a bound electron

Summary

1. Photon vortices are naturally generated in the universe.

2. We have calculated the photon vortex generation in extremally strong magnetic fields such as magnetars or black holes.

   T. Maruyama, T. Hayakawa, M.K.Cheoun, T.Kajino, PLB826, 136779 (2022)

3. We have calculated the photon vortex generation by nonlinear Compton scattering with high power laser.

   T. Maruyama, T. Hayakawa, M.K.Cheoun, T.Kajino, ApJ 975, 51 (2024)

4. We have calculated the transition probability ratio of the photon vortex to the plane wave in photon nucleus interactions.

5. When we control the impact parameter in order of wavelength, we can observe the difference, but the total cross sections are identical.

   T. Maruyama, T. Hayakawa, M.K.Cheoun, T.Kajino, Phys. Rev. D 111, 016016 (2025).

The 6th Nuclear Photonics Conference

Nara, Japan, Sep. 27- Oct. 1, 2027

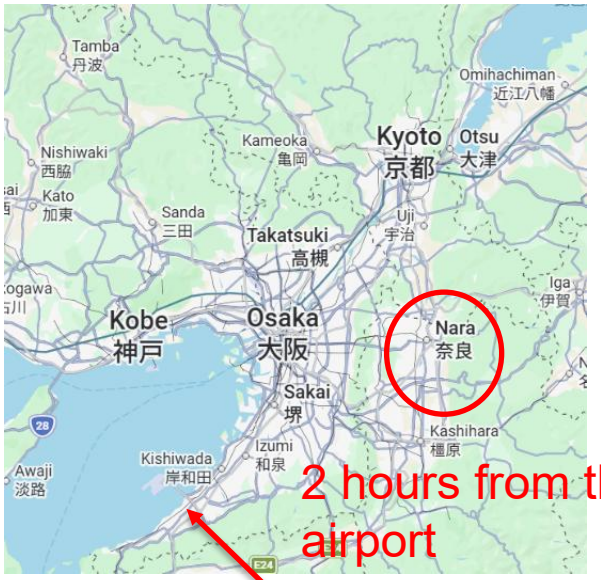
Fundamental nuclear science and spectroscopy with photons
Laser–plasma nuclear physics
High intensity laser–plasma interaction
Photon nuclear science
Laser Compton scattering gamma-ray sources and its applications
Medical applications using laser-driven particles and photons
Industrial applications using high power laser and photons such as imaging
Nuclear astrophysics and stellar nucleosynthesis such as r-process
Strong field QED,
etc.

Chair: Ryoichi Hajima

- Monterey, CA, USA (2016)
- Brasov, Romania (2018)
- Osaka, Japan (2021)
- Durham, NC, USA (2023)
- Darmstadt, Germany (2025)

Nara Centennial Hall
https://www.nara100.com/index.html







https://www.advantour.com/img/japan/nara/nara-park-deer.jpg
Source: www.advantour.com

Many historical spots in Japan within a 30-min. walk

Nara Central hall locates at the center of Nata city and 5 min walking from the JR Nara station

